SYNTHESIS AND CHARACTERIZATION OF AMORPHOUS ALUMINA AND ITS ELECTROPHORETIC DEPOSITION FROM POLYACRYLIC-ACID AQUEOUS SUSPENSION

by

VIKAS KAUSHIK

DEPARTMENT OF METALLURGICAL ENGINEERING

INDIAN INSTITUTE OF TECHNOLOGY KANPUR

AUGUST, 1982

SYNTHESIS AND CHARACTERIZATION OF AMORPHOUS ALUMINA AND ITS ELECTROPHORETIC DEPOSITION FROM POLYACRYLIC-ACID AQUEOUS SUSPENSION

A Thesis Submitted
in Partial Fulfilment of the Requirements
for the Degree of

MASTER OF TECHNOLOGY

by

VIKAS KAUSHIK

to the

DEPARTMENT OF METALLURGICAL ENGINEERING
INDIAN INSTITUTE OF TECHNOLOGY KANPUR

AUGUST, 1982

DEDICATED TO MY SISTER

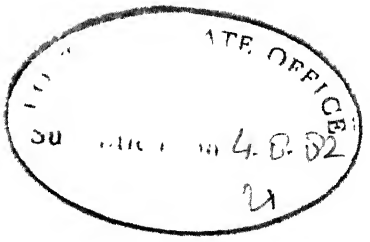

CERTIFICATE

This is to certify that the thesis entitled 'SYNTHESIS AND CHARACTERIZATION OF AMORPHOUS ALUMINA AND ITS ELECTROPHORETIC DEPOSITION FROM POLYACRYLIC ACID AQUEOUS SUSPENSION', submitted by Mr. Vikas Kaushik, in partial fulfilment of the requirements for the Degree of Master of Technology at the Indian Institute of Technology, Kanpur is a record of bonafide research work carried out under my supervision. The work embodies in this thesis has not been submitted elsewhere for a degree.

(Dr. K.N. Rai)
Assistant Professor
Department of Metallurgical Engg.
and Material Science Programme
Indian Institute of Technology,
Kanpur

Indebted to

Dr. K.N. Rai, thesis supervisor

Dr. H.S. Ray

Dr. Jitendra Kumar

Thankful to

Mr. Ashok Kumar,

Mr. Narinder Pal Singh,

ACMS people and a lot of friends, who cheered me up during this work.

Vikas Kaushik

CONTENTS

PREFACE

Coatings based on refractory compounds are currently finding ever increasing application in various branches of industry and technology for the protection of components, subjected to high temperatures and corrosive environment. This work concerns about development of amorphous alumina and polyacrylic acid (polymer) for their possible use in protective coating by process of electrophoresis through aqueous medium.

The Chapter 1 is a short review on the various methods of coating with reference to refractory materials. The Chapter 2 describes the synthesis, characterization and phase transformations of amorphous alumina. The synthesis and characterization of polyacrylic acid (polymer) has been discussed in Chapter 3. The Chapter 4, describes the result of exploration of the above synthesized materials for the use in electrophoretic coating. In the last the work is concluded.

List of Figures

List of Tables

Chapter 1

REFRACTORY COATINGS

Abstract

Since long metallurgists are facing problem of protecting engineering materials from high temperature oxidation and environmental deterioration. Consequently the coatings of high temperature materials have been used extensively as a protective tool. The present chapter briefly reviews art and techniques of coating with special reference to coatings of refractory materials.

1(A)

INTRODUCTION

Applications of high temperature materials in the form of coatings is of great technological interest on metallic and non-metallic materials. In a number of cases, the production of such coatings is most effective and sometimes it is the only method of imparting special physiochemical properties such as wear resistance, resistance to corrosion and high temperature oxidation to the surfaces of components.

The coating should act as an air barrier; it should be ductile and the process of coating should gurantee a

perfect continuity of the coated layer. Physical and chemical stability of the coated layer is a prime factor in coating technique. The problems of bonding between the material to be coated and the coated layer are not simple. There are only a few of the aspects which have been received attention during the last few years. The results of the coating investigation for space technology purposes, however, have found many other applications in the other fields of technology where materials are exposed to high temperature. 15

The important objectives of high temperature materials coatings are to control oxidation or diffusion, emittance and conductive heat transfer and to have erosion or abrasion resistance. Most coatings serve more than one of the above functions, and overall performance is always a compromise. For high temperature oxidation resistance, a coating should resist oxygen and metal ion diffusion and should have a low vapour pressure at the operating temperature, a melting point above the operating temperature and low reactivity with the substrate and environment.

Coatings for mechanical protection, thermal conductivity, and emittance control represent an important segment of current efforts. Generally, the internal chemistry and reaction mechanisms within the coating-base system are less important than the external characteristics. The primary concern is generally the adhesion, hardness and toughness of the coating.

For emittance control, however, only the external characteristics are important. The reaction mechanisms in or on the surface of coating.and vaporization of coating which destroys the desired surface need to be given due consideration. Since emittance characteristics vary with the surface roughness, the application technique is also an important variable.

1(B)

ADHESION OF COATINGS

A prime consideration in coating technology is adherence. In many of the potentially interesting coating substrate systems, the transition from the substrate material to the coating usually involves an abrupt change in such properties as hardness, coefficient of thermal expansion and thermal conductivity.

Much experimental work has been performed on adherence, and numerous theories or explanations for interface bonding have been presented [15]. In generalizing, the explanations rely on factors such as mechanical interlocking, epitaxial overgrowth, mutual wetting or mutual solution of constituents at the interface, chemical reaction and diffusion. For each coating system, the importance of each factor varies. For example, Ault and Wheildon [1] realized that flame spray coatings did depend largely on mechanical interlocking for

attachment to the substrate and interlocking of individual particles. In applying siliconized coatings, diffusion and reaction to form new compounds at the surface or interface are largely responsible for coating adherence. The coating in this case has no abrupt end, but exhibits a smooth transition into the base metal. For sintered or vitreous coatings, adherence depends on coating reaction with the surface oxide, (or the metal) and solubility of the metal (or oxide) in the coating.

Many tests do not exactly distinguish between the extent of interface adhesion and cohesive strength of the coating. Impact tests, frequently measure largely the strength of the coating material under a rapid, complex loading. A weak coating material might fail, with many particles adhering to thebase metal, and be evaluated as having excellent adherence. On the otherhand a very strong coating material with actually better interface adherence could fail at the interface, parting clearly from the metal, and be evaluated as having 'poor' adherence because there was little evidence that coating particles remained on the surface.

Stresses are inevitably produced at the coating-substrate interface during the cooling-down period after deposition and during service because of differences in thermal properties. In addition, higher internal stresses tend to built up in

thick coatings. The concentration of these permanent and transient stresses leads to a reduction of bonding strength, which in turn may lead to cracking or splitting of the coating from the substrate. The end result is a shorter service life. Various ways and means have to be used to reduce these stresses and to increase the adhesion between the coating and the substrate.

The more common methods [16] for reducing stresses are:

(i) matching the properties of coating and substrate.

(ii) forming intermediate layers to reduce the large gradient of properties between the coating and the substrate.

(iii) controlling the structure of the coating.

(iv) reducing the coating thickness.

(v) increasing the radius of currature of the coated surface.

The precise influence of internal stresses on the adhesion in real coating-substrate systems is not known, although this effect in an idealized system has been recently investigated by Wahl [17]

The matching of coefficients of thermal expansion is often required in protective coatings because thermal expansion has a very large effect on stresses. Whether the internal stresses caused by thermal expansion differences are destructive to the coating integrity, depend on their magnitude. The additional stresses from the thermal gradients across the coating, and the ability of the base, interface of coating to deform plastically also determines the state of coating.

The thermal shock resistance is less of a problem at temperatures above 1200°C than at or near room temperature, because even the brittle oxides, hard metals and intermetallics exhibit some plastic deformation at high temperatures and this deformation, though small, can provide some stress relief. In addition, the modulus of elasticity of most materials decreases with increased temperature and the lower modulus of elasticity of the coating materials reduces the induced stress level. To calculate the stress in a coating-base system, it is also necessary to know the modulus of the composite as a function of temperature. The conclusions of several investigations (5) indicate that for brittle coatings, the thermal shock resistance can be increased by introducing moderate residual compression stresses into the coating at low temperatures. Decreasing the thickness of the coating also improves the thermal shock resistance.

Thermal shock resistance is closely allied with the absolute values of thermal expansion, the mechanical properties of the coating and base, and the thermal conductivity of the coating and substrate. In general, the thermal stress resistance (R) of a body can be related to the mechanical and thermal properties. It is proportional to the maximum temperature gradient to which a brittle body can be subjected without

fracturing. Thus,

$$R \simeq \frac{S\,(1-\mu)}{E\alpha}$$

$$R' \simeq \frac{S\,(1-\mu)K}{E\alpha}$$

where S = strength

μ = poission's ratio

E = modulus of elasticity

α = thermal expansion

K = thermal conductivity of the material

R and R' are I and II thermal stress resistance factors respectively.

1(C)

COATING METHODS

Numerous methods are available for applying coating materials to a given substrate. Each of them have its own merits and demerits depending upon the end application. These methods are Spraying, Cladding, Vapour deposition, Enamelling, Vacuum metallizing, Hot-dipping, Slurry methods, Methods based on Exothermic reactions, Electrolytic and Electrophoretic deposition.

Spraying Methods

The two basic processes of spraying materials for high temperature coatings are flame spraying and arc-plasma spraying. Spraying in both these processes involve three stages.

(i) heating the material to be sprayed to form molten or semimolten droplets in a flame or plasma.

(ii) projecting these heated particles at a high velocity onto the part being coated, and

(iii) the collision of the hot particles with this part, where they adhere to the substrate to form the final coating.

Cladding Methods

It is an ideal method of reliably applying a continuous chemically and metallurgically sound coating layer of metal to sheets, rods and other objects of simple shape. To accomplish cladding, most common technique is to capsulate the base metal with the cladding material and roll or forge while hot. The paramount limitation of this technique is the simple shape requirement. The important metallurgical limitations are diffusion, bond strength, the formation of low-melting alloys or brittle intermetallics.

Vapour Deposition Method

It is the technique in which the coating material is carried in the gaseous state to a heated substrate whereon the coating material is deposited, the gas vehicle going off as a waste product. The mechanisms by which the coating element is deposited, are chemical reduction, condensation, pyrolysis or thermal decomposition and displacement.

Electrodeposition

It is the most widely used method of applying protective metal coating to another material either from aqueous solutions or from fused salts. Electro-deposition of cermets from aqueous solutions has been investigated for high temperature coating applications on metals and graphite [11, 13]. Hirakis [15] has described the electrodeposition of nickel-base cermets for columbium. Chromium-base cermets [11, 13] may be coated on the refractory metals and graphite using Zirconium and tungsten borides, Zirconium nitride and molybdenum carbide as the particulate materials.

Metal-ceramic coatings containing a variety of oxide and hard metal particles have been prepared. Nickel, chromium, platinum, rhodium and cobalt-tungsten have been used as metallic phases [13]

Plating from fused salt solvents is commonly used for the electrowinning of metals, but some investigations are done for high temperature coatings also. Hirakis [15] has deposited titanium, chromium and aluminium for the protection of columbium and molybdenum from fused salts. He found that coatings of titanium and aluminium were easily obtained, but that the complete coverage of the specimen with chromium was impossible, particularly in the area of cathode contact.

Electrophoretic deposition

In addition of the above described techniques, the electrophoretic deposition is also a significant technique for the coating on conducting substrate. This method of coating depends on the phenomenon of electrophoresis, which may be defined as the movement of charged particles in a suspension on passing electricity. It has been dealt in detail in Chapter 4.

Enamelling methods

Enamel coatings are prepared by proportioning the frit composition, mixing and heating to melting. The melt is then poured into water or quenched rapidly and is thus broken into small fragments. The frit is then ready to blend for a coating and may be used above or with crystalline materials added to make a more refractory coating. Common additions are ZrO_2, Al_2O_3, Cr_2O_3, Cr and clays.

The coating is applied by dipping the substrate in the slip or painting or spraying the slip on the substrate. After air-drying (sometimes further drying by heating upto 260°C), coating is vitrified by firing to a temperature depending upon frit mixture composition for periods of 1 to 30 minutes.

Vacuum metallizing

The coating metal is heated on a spiral helix (or in a boat of a refractory metal, a ceramic crucible, or by other suitable methods) to a temperature at which its vapor pressure is significant. The vapor then condenses on any cool substrates placed in the vacuum chamber. Adherence, in this technique, is very poor unless the substrate is heated during evaporation. The method is very inefficient, because the evaporating metal is condensed onto all areas of the coating chamber and only a small amount falls on the substrate.

Hot dipping methods

There are three dipping techniques used to apply coatings for high temperature use; simple dipping of substrates in molten metals, dissolution from molten metals, and dipping in fused salts. The application of coatings by dipping the substrate in a molten metal is widely used. Well known examples are dipping steels in molten zinc or aluminium. Hot dipped coatings are normally applied by placing the substrate in a molten bath of the coating material.

The principle of Selective Freezing (Desolutionizing) for deposition is applicable to the systems in which the plating metal and base metal are isomorphous, form no intermetallics during the deposition process, and in which the coating metal is soluble in a low-melting metal solvent.

Slurry method

Applying coatings by the slurry method consists of blending the coating composition in powder form, suspending the powders in a liquid carrier to make a slurry and painting, dipping, or spraying the coating slurry on the substrate. After the suspension has air-dryed, it is diffused into the substrate by heating in an inert atmosphere or vacuum.

Methods based on exothermic reaction

The general reaction is

$$MO_x + A \longrightarrow AO_x + M$$

where M represents a metal whose oxide has a free energy of formation less than that of the oxide AO_x. A is commonly aluminium and AO_x is aluminum oxide. Other coating reactions, which are referred to as thermite reactions, are as follows -

$$SiO_2 + MO_x + Al \longrightarrow Al_2O_3 + MSi_x + MO_x$$

$$B_2O_3 + MO_x + Al \longrightarrow Al + Al_2O_3 + MB_x$$

$$C + MO_x + Al \longrightarrow Al_2O_3 + MC_x$$

Coatings are produced via these reactions by mixing the starting powders in a slurry and applying to the substrate, the

reaction is initiated by heating to a temperature of about 1100°C.. Heat is a byproduct of the reaction and surface temperatures of 2800°C are not uncommon, hence the name exothermic reactions.

1(D)

MATERIALS & CHARACTERISTICS OF HIGH TEMPERATURE COATINGS

The main high temperature coating materials are refractory oxides, the hard metals (carbides, borides, nitrides, silicides), the intermetallics, the metals and the pyrolytic deposits.

The refractory oxide materials are characterized by stability in an oxidizing atmosphere, high melting point, high compressive strength, a brittle failure at low temperatures, and low or moderate cost. The oxide systems provide the basis for the ceramic, glass and refractory industries. The structures of most oxide crystals are much more complex than the metal and semi conductors.

Alpha aluminium oxide is one of the most widely used refractory compounds, which possesses high mechanical strength. It's melting point and vapour pressure are 2048°C and less than 1 torr at melting point respectively. It possesses excellent stability above 1700°C, even in a strongly reducing atmosphere.

The oxide film formed on aluminium is protective against continued oxidation; however the low melting point of the metal precludes its use alone as a high temperature coating material.

Impure aluminium oxide and aluminates are also the protective oxidation products of the aluminide intermetallics. Since the melting point of many aluminium oxide coatings in situ through the oxidation of aluminide coatings has provided a practical method of applying alumina in coating form.

Beryllium oxide is a stable oxide and has low volatility with a melting point of 2571°C, higher than that of alumina. Its high electrical resistivity, low electrical loss and low density make it often more attractive than alumina as an electrical insulator, particularly for use at very high temperature (1700-2000°C). These characteristics show its merits as refractory material, but eventhen due to its toxicity it can not be used freely.

Cerium oxide is an inert and valuable refractory oxide for general use. As an addition to Zirconia, it stabilizes the cubic structure. But CeO_2 is rarely used for this purpose due to its high cost. Ceria is readily flame-sprayed, forming a dense coating. Since partial reduction may occur during applications, the resulting oxygen deficiency in the coating structure may improve the short-term oxidation protection provided by ceria coatings.

Chromium oxide, which is rarely used alone, has wide usage in combination with MgO for chrome-magnesite refractories for the steel industry. A number of high temperature coatings for ferrous alloys contain Cr_2O_3 in high percentages and oxides

from many Ni-Cr alloys (containing Cr_2O_3) offer appreciable oxidation protection to the base alloy.

Hafnium oxide is easily flame or plasma-sprayed and the resulting coating is similar to those formed from Zirconia. However, hafnium metal is not protected by HfO_2 and oxidizes rapidly at high temperature.

1(E)

COATINGS ON GRAPHITE

Graphite is one of the promising high temperature constructional materials because of its low specific gravity and easy machinability. It possesses high thermal conductivity, a low coefficient of thermal expansion and relatively satisfactory strength, upto 2700°C. However because of its low resistance to oxidation and abrasive wear in a current of hot gases and considerable rate of evaporation at high temperatures, it can not be used without providing a protective coating.

Graphite can be protected either by carbide coatings or by metallic coatings. Carbide coatings may be deposited by thermal diffusion treatment with refractory metals, silicon or boron. This process is carried out in the gas phase, using halides, carbonyls, or organic compounds of above mentioned saturating elements. A carbide film may also be produced by wetting the surface of the graphite with liquid metal, or flame spraying. At a sufficiently high temperature, specific for each metal, the metal coating is converted into a carbide coating 15 .

To apply metallic coating to graphite specimen, a suspension of a solution of polystyrene in an organic solvent having suspended particles of the finely divided metal or its compound is deposited. The volatile contents of the suspension are then removed by heating the article in a high vacuum. The organic substances are partly evaporated, but are mainly converted into pure spongy carbon, forming an intermediate layer between the graphite and the metallic layer. A tungsten coating, applied by means of a plasma arc directly to the surface of the graphite nozzles of the rocket engine, protects them from the erosion effects of combustion products having high temperatures and velocities. Plasma spraying ensures high density of the coating and its firm bonding to the base 15 .

Graphite-moderators of an atomic reactor have been protected from high-temperature oxidation by producing a coating of silicon. At first, silicon powder is applied to graphite, which is followed by melting of silicon film by local heating of a portion of the surface of the body without heating the entire graphite mass. The molten spreads over the surface and on reaction with carbon, forms silicon-carbide. Due to high resistance of silicon metal, it is not necessary to convert whole silicon into silicon carbide. An another method for applying coating to graphite comprises the decomposition of silicon organic compounds of the type of methylchlorosilanes (di- & tri-), in which the molecule contains an equal number of

carbon and silicon atoms. Thermal decomposition of these compounds at 1100-1500°C gives dense and homogeneous layers of SiC being formed in a hydrogen atmosphere. One interesting method of applying composite coating on graphite articles is to coat metal carbide & nitride in one stage.

REFERENCES

1. Ault, N.N., and Wheildon, W.M.; "Modern Flame Sprayed Ceramic Coatings", chapter in "Modern Materials", H.H. Hausner, Ed., New York, Academic Press, Inc., 1960.

2. Timoshenko, S., "Theory of Elasticity", New York, McGraw Hill Book Company, Inc., 1934.

3. Walton, J.D., Jr., "Study of Strains Between Enamel and Iron as Related to Physical Properties of Each", J. Am. Ceram. Soc., 37, No. 3, 153 (1954).

4. Cown, R.E., at el., "Effect of Temperature on Modulus of Elasticity of Porcelain Enameled Steels", J. Am. Ceram. Soc., 39, No. 9, 293 (1956).

5. Timoshenko, S., "Theory of Elasticity", New York, McGraw Hill Book Company, Inc., 1934.

6. Hardwood, J.J., "The Protection of Molybdenum Against High Temperature Oxidation", 43rd Proceedings of Am. Electroplaters' Soc., 1956.

7. Brenner, A., and Associates, "Protection of Molybdenum From Oxidation at Elevated Temperatures", J. Electrochem. Soc., 108, 450 (1958).

8. Safranek, W.H. and Schaer, G.R., "Properties of Electrodeposits at Elevated Temperatures", 43rd Proceedings of Am. Electroplater's Soc., 1956.

9. Brenner, A. and Associates, "The Use of Nickel Aluminium Alloy Coatings for the Protection of Molybdenum From Oxidation", J. Electrochem. Soc., 108, 485 (1958).

10. Reid, W.E. and Ogborn, F.J., "The Adhesion of Electrodeposited Nickel to Chromium at Elevated Temperatures", J. Electrochem. Soc., 107, 91 (1960).

11. Withers, J.C., "Electrodepositing Cermets", Products Finishing, 62 (Aug. 1962).

12. Withers, J.C., "Electroplated Cermet Coatings for Oxidation Protection of Substrates in Excess of 2000°F", WADD-TR 60-71

13. Huminik, John, "Development of Oxidation and Erosion Resista Coatings for Mo, Ta and W", Contract DA 36-034-ORD-327 ORD, March, 1961.

15. Samsonov, G.V. et al., "High Temperature Materials, Plenum Press, N.Y. 1966.

16. Blocher Jr., J.M.; ibid, 11, 680 (1974).

17. Wahl, G.; Z. Werkst. Tech., 7, 311 (1976).

Chapter 2

SYNTHESIS, CHARACTERIZATION, PHASE TRANSFORMATIONS AND SINTERING OF AMORPHOUS ALUMINA

Abstract

Amorphous alumina powder has been synthesized from the hydrolysis of aluminium isopropoxide and subsequent dehydration. The dehydration process has been explored using DTG, DTA and TG techniques. The phase transitions in amorphous alumina has been studied using X-ray diffraction and electro microscopy. The sintering behaviours such as increase in density with temperature and time and associated activation energy have also been evaluated. Finally the compressive fracture strength of alumina pellets, sintered upto 1400°C, has been studied.

2(A)

INTRODUCTION

Ceramists have always been interested in obtaining high purity ultrafine ceramic powders ($<1\mu$) for the preparation of high density ceramic bodies. Reason of interest being the large surface area of fine particles which helps in sintering to dense bodies almost reaching the theoretical density at substantially lower processing temperatures. Coating technologists are also equally eager to have ultrafine powder for smooth and coherent coatings.

A variety of techniques for the preparation of ultra-fine ceramic powder involves a liquid solution of metallic salts as an initial step, which is followed by the removal of the solvent. The solvent removal leaves a residue which is the final powder. In many cases, residue has to be calcined to obtain the final product.

The solvent can be removed by (i) solvent vaporization, (ii) solution combustion or (iii) by precipitation-filteration.

In solvent vaporization, the solute is separated from solution by removing the solvent as vapour phase. Direct evaporation may be suitable for single-component solutions. With multi-component solutions, large-scale segregation of the components often results. Spray-drying prevents segregation during evaporation by breaking the liquid into very small droplets. This promotes rapid evaporation to minimize segregation and assures that any segregation is confined to the small droplets, since no mass transfer from droplet to droplet takes place.

The solution combustion encompasses those preparation techniques, in which solutions are actually burnt to form solid particulates. It also includes to some extent those techniques that volatilize liquids for hydrolysis, decomposition, or oxidation from the gaseous state.

The precipitation with subsequent removal of the solids by filteration is one of the most widely used techniques for the preparation of ceramic powders from solutions. This involves a large number of variables like pH, solution concentration, temperature, atmosphere which can affect the process.

While most precipitations are affected by the solution of a precipitating ion, the addition of an aqueous solution to a large excess of a second solvent in which the original solute is insoluble will also cause precipitation to occur. This principle forms the basis for a powder preparation technique termed as 'liquid drying'. 3

Earlier workers have synthesized alumina from chlorides, nitrates and by the use of other inorganics. Later preparations are based on the alkoxide process, which mainly involves three steps viz. preparation of alkoxide, its hydrolysis to yield aluminium hydroxide and finally dehydration.

Hydrolysis, depending upon actual process, has been found to yield three different varieties of aluminium hydroxide (hydrated alumina) known as Gelatinous aluminas. These are (i) X-ray indifferent (amorphous), (ii) gelatinous boehmite and (iii) trihydroxide.

Torkar and Egghart 6 have synthesized a X-ray indifferent alumina by the hydrolysis of $Al(O\ C_2H_5)_3$ at 0°C. X-ray indifferent alumina was also prepared by Teichner 9 from aluminium methylate.

Fricke and Jockers 18 have obtained alumina by hydrolyzing aluminium alcoholates at temperatures below 40°C.

Amalgamated aluminium was used for the preparation of crystalline alumina by Watson et al 7 and Schmah 20 . Watson et al used ammonium alum and got sols and gels.

Turkevich and Hiller 8 precipitated spherical particles combined with fibers from aluminium nitrate and ammonia. Teichner 9 and Papee et al 10 also obtained gels from ammonia ad aluminium nitrate of various pH.

Harris and Sing 11 formed by interaction of sodium hydroxide and Al-salt solutions, and by hydrolysis of aluminium isopropoxide.

A fibrous gelatinous boehmite has been described by Bugosh 15 . This material is precipitated in an acid environment. It is a very fine crystalline powder which forms a gel when mixed with water.

Transparent films of highly oriented pseudoboehmite have been prepared by Milligan & Weiser 16 by evaporating a thixotropic sol to dryness at room temperature. These films remained transparent and oriented after being transformed into a transition alumina by heating to about 700°C.

Bayerite (aluminium trihydroxide) has been prepared by treating $AlCl_3$ solutions with cold NH_4OH, followed by aging at room temperature Neutralization of a sodium aluminate

solution with CO_2 at 20°C. (Fricke and Wullhorst 17) or autoprecipitation at low temperature from aluminate solution also lead to the formation of bayerite.

Torkar and Bergmann 19 produced extremely pure bayerite electrolytically, using Pt cathodes, Al-anodes and H_2O as an electrolyte.

Tremper et al 22 developed a low temperature process for the production of high purity aluminium oxide powder. This process consists of converting in an autoclave high purity (99.9%) aluminium metal directly to the oxide at low temperatures (300-500°C) and moderate steam pressures (500-5000 psi).

All the hydroxides are converted to pure alumina after dehydration of hydroxides (including gelatinous alumina) above 300°C.

2(B)

SYNTHESIS OF AMORPHOUS ALUMINA

Synthesis of alumina can be carried out from aluminium alkoxide, preferably aluminium isopropoxide. In general, metal alkoxides with formula $M(OR)_n$, where M is the metal and R, any alkyl group (e.g. C_2H_5, C_3H_7, C_4H_9 etc.), can be easily synthesized and can be converted into metal oxides either by thermal degradation or hydrolyzation followed by dehydration as:

$$M(OR)_n \xrightarrow{\text{Thermal degradation}} MO_{n/2} + n/2\ ROH + \text{Alkene}$$

$$M(OR)_n \xrightarrow{\text{Hydrolyzation}} M(OH)_n + n\ ROH$$

$$M(OH)_n \xrightarrow{\text{Dehydration}} MO_{n/2} + n/2\ H_2O$$

Generally the above reactions take place below 500°C and the product consists of unusually small particles of size typically around 100 A°.

(a) Synthesis & Characterization of Aluminium Isopropoxide

Aluminium isopropoxide was synthesized by the method developed by Aldkin [22].

Aluminium turnings were taken in reaction vessel with isopropyl alcohol and then $HgCl_2$ was added as a catalyst.

All materials, taken, were perfectly free of water and during the reaction the apparatus was adjoined with a drying tube containing $CaCl_2$ to protect the reaction mixture from moisture. The metal got dissolved in the alcohol at reflux

temperature (85°C) in a period of 4 to 6 hours. After completion of reaction, the excess of alcohol was distilled off (b.p. of isopropyl alcohol = 82.4°C) and the aluminium isopropoxide was taken out of the reaction flask.

The set up used for this synthesis is shown in Figure 2.1. The amounts of the reactants were taken as follows:

Al turnings	12.75 gms.
Isopropyl alcohol	100 ml. (approx.)
Mercuric chloride	0.27 gms.

During refluxing, the following reaction occurs:

$$2\ Al + 6\ C_3H_7OH \longrightarrow 2\ Al(OC_3H_7)_3 + 3\ H_2$$

The $HgCl_2$ acts as a catalyst for providing clean Al surface for reaction by amalgamation.

$Al(OC_3H_7)_3$ decomposes on exposure to moisture forming $Al(OH)_3$ and alcohol. For storage, therefore, Isopropoxide container was tightly closed.

(b) Infrared Characterization of Isopropoxide

Infrared studies of the synthesized aluminium isopropoxide was carried out on Perkin-21 spectrometer. The observed spectrum was compared with the standard spectrum, given by Bell et al [23].

For isopropoxy group, characteristic absorptions were found to occur at 8.5 (1125 cm^{-1}), 8.8 (1135 cm^{-1}) and 9.0 (1110 cm^{-1}) microns. These bands were found to be present in IR spectra of all metal isopropoxides analyzed by Bell et al.

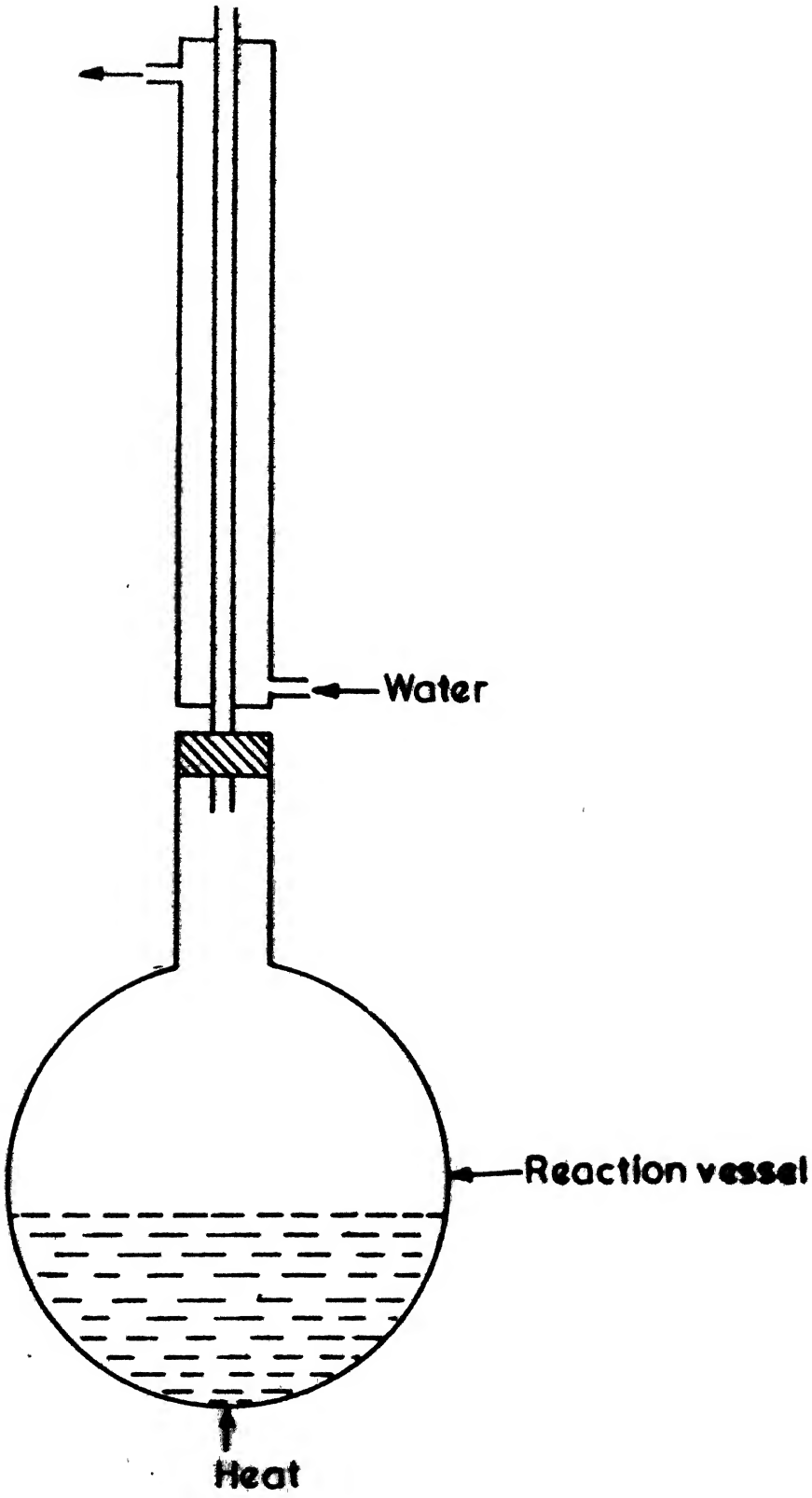

Fig. 2.1. Setup for synthesis of Aluminium Isopropoxide.

In the case of isopropoxy absorption bands, the 8.5 micron band had been identified as characteristic of iso-branching [24,25]. The 8.8 micron band was thought to be an alkyl absorption induced by the proximity of the oxygen atom. The intensity of the 9.0 micron band suggests that it is essentially an oxygen to carbon stretching absorption [26]. The spectrum demonstrates a slight hydroxyl absorption in the 2.8 to 3.2 micron region. This is due to a very small amount of hydrolysis, as all these compounds are hygroscopic and subject to hydrolysis.

The observed spectrum is compared with that of standard spectrum in Table 2.1. The region of the spectrum in the range 6 to 16 microns, which represents the most characteristic absorption peaks of the compound, are given in the Figure 2.2. It is observed that the values of present sample are matching pretty well with the standard [illegible]. Because of low resolution in [illegible] wave length region, the peaks appear as a broad band.

(c) Synthesis of Alumina

The aluminium hydroxide, obtained by hydrolyzing in distilled water was heated at 100°C for 4-6 hours to eleminate external water and isoprolyl alcohol, which result during hydrolysis as indicated below.

$$Al(OC_3H_7)_3 + H_2O \dashrightarrow Al(OH)_3 + C_3H_7OH$$

The dried aluminium hydroxide was further calcined at about 400°C for overnight. This yielded amorphous alumina as follows:

$$Al(OH)_3 \xrightarrow{\text{About } 400^\circ C} \underset{\text{Amorphous alumina}}{Al_2O_3} + H_2O$$

Table 2.1

Infrared Absorption Data of Aluminium Isopropoxide

(Wavelength in microns)

Data from Bell et al 23	Present data
3.39	3.4
3.43	3.4
	3.45
3.52	3.5
3.82	4.6
	5.3
	5.7
6.83	6.8
7.20	7.1
7.28	7.3
7.35	7.35
7.40	
7.50	7.5
8.03	7.7
8.29	8.6
8.48	8.7
8.55	8.8
8.82	
8.92	8.9
9.69	9.7
	9.8
	10.0
	10.25
	10.3
10.55	10.5
11.64	
11.98	12.0
	12.4
13.00	
14.32	
14.80	

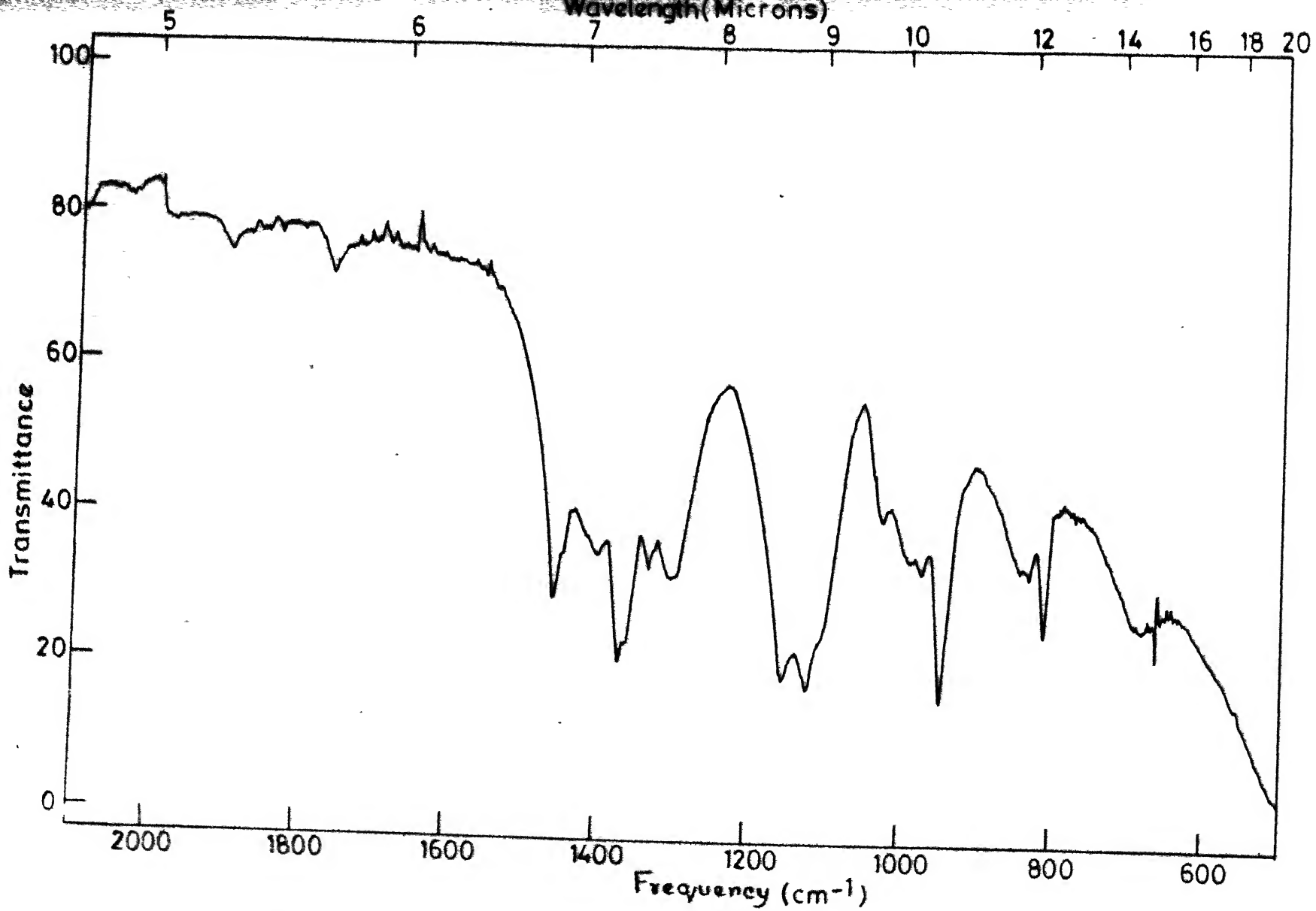

Fig 2 2 Infrared absorption spectrum of $Al(OC_3H_7)$.

2(C)

PHASE TRANSFORMATIONS IN ALUMINA

In order to investigate phase transformations, dehydrated aluminium hydroxide powder was fired at 200°C, 300°C, 400°C, 500°C, 600°C, 700°C, 800°C, 900°C, 1000°C, 1100°C, 1200°C, 1300°C and1400°C for 6 hours each in ambient atmosphere. These temperatureswere umaintained constant to an accuracy of $\pm$ 10°C.

(a) X-ray diffraction studies

X-ray diffraction patterns of the samples, fired on different temperatures, as mentioned above, were obtained with CuK_{α} radiation (tube voltage 45 KV and tube current 15 mA) with Ni filter using GE-XRD-6 diffractometer at 500 cps (time constt. 4 sec.) and at a scanning rate of 2° (2θ)/minute.

The d_{hkl} values were calculated using Bragg's Law and were compared with standard ASTM data for aluminium hydroxide and different forms of alumina, as shown in Table 2.2, 2.3 & 2.4.

Following significant observations were made:

1. The hydroxide exists mainly in boehmite form and it starts slowly dissociating above 300°C and completely dissociates till 500°C is reached.

2. The dissociated product was amorphous alumina. It stays as such upto 700°C.

Table 2.2. Comparison of d-values

ASTM data (prepared by Swanson & Fuyat) [1]		Experimental data			
		Fired at 300°C (Boehmite)		Fired at 400°C (Boehmite)	
$d_{(A°)}$	I	$d_{(A°)}$	I	$d_{(A°)}$	I
6.11	100			6.147	06
3.164	65	3.129	08	3.119	10
2.346	53	2.466	10	2.307	10
1.980	6				
1.860	32				
1.850	27	1.850	13	1.843	11
1.770	6				
1.662	13				
1.527	6				
1.453	16				
1.434	9	1.433	05	1.429	04
1.412	1				
1.396	2				
1.383	6				
1.369	2				
1.312	15	1.310	03		
1.303	3				
1.224	1				
1.209	2				
1.178	3				
1.171	1				
1.161	3				
1.134	5				
1.092	1				
1.046	2				

(Samples fired at 500°C & 600°C show no peaks.)

Table 2.3 Comparison of d-values

Data quoted in literature [1]						Experimental data					
Chi-alumina		Gamma-alumina		Eta-alumina		Fired at 700°C (Evolution of Chi or Gamma or Eta alumina		Fired at 800°C (Evolution of Chi or Gamma or Eta alumina		Fired at 900°C (Evolution of Chi or Gamma or Eta Alumina	
$d_{(A°)}$	I	$d_{(A°)}$	I	$d_{(A°)}$	I	$d_{(A°)}$	I	$d_{(A°)}$	I	$d_{(A°)}$	I
2.40	4	2.7	2	4.6	4						
2.27	2	2.41	6	2.8	2						
2.11	3	2.28	6	2.40	6					2.402	06
1.98	2	2.18	2	2.27	3						
1.53	1	2.09	1								
1.39	10	1.98	10	1.97	8	1.979	-	1.979	07	1.979	09
		1.95	6								
		1.54	2	1.52	2						
		1.39	10	1.40	10	1.395	-	1.399	12	1.401	13
				1.21	1						
		1.14	3	1.14	2						
		1.04	1	1.03	1						

Table 2.4. Comparison of d-values

α - alumina

ASTM data for α - alumina		Experimental data					
		Fired at 1000°C		Fired at 1100°C		Fired at 1200°C	
$d_{(A°)}$	I	$d_{(A°)}$	I	$d_{(A°)}$	I	$d_{(A°)}$	I
3.479	74	3.4509	31	3.4635	35	3.4649	30
-	-	2.8376	05	-	-	2.8465	04
2.552	92	2.5404	55	2.5474	59	2.5404	51
2.379	42	2.4211	15	2.4274	14	2.4274	14
2.165	1	2.3719	26	2.3779	26	2.3719	24
2.085	100	2.0786	65	2.0832	74	2.0786	62
1.740	43	2.0127	09	2.0213	10	2.0127	09
1.601	81	1.7354	34	1.7385	39	1.7385	26
1.546	3	1.5988	60	1.6014	73	1.5988	58
1.510	7	1.5522	08	1.5546	10	1.5522	09
1.404	32	1.5087	05	1.5106	07	1.5087	05
1.374	48	1.4257	11	1.4277	14	1.4257	12
1.276	2	1.4029	13	1.4048	32	1.4029	24
1.239	16	1.3721	25	1.3739	48	1.3721	34
1.190	6	1.2346	11	1.2373	15	1.2359	12
1.160	1	1.1884	03	1.1909	04	1.1884	03
1.147	4	1.1456	02	1.1467	02	1.1456	02
1.138	1	1.1231	03	1.1252	04	1.1231	03
1.125	5	1.0970	03	1.0989	04	1.0980	04
1.099	6	1.0780	05	1.0790	06	1.0771	05
1.088	3	1.0431	09	1.0439	-	1.0422	09
1.078	7	0.9982	06	0.9982	10	0.9982	07
1.043	13			0.9335	03	0.9335	03
1.018	1						
0.998	11						
0.982	2						

Table 2.5. Calculated Lattice Parameters of χ-Alumina

d in A°	hkl	c	$\frac{4}{3}(\frac{h^2+hk+k^2}{a^2})$	a	d calculated
3.4509	012	-	0.0590	12.6744	3.4523
2.8376	-	-	-	-	-
2.5404	104	-	0.590	12.9167	2.4470
2.4211	-	-	-	-	-
2.3719	110	4.7437	0.1772	-	-
2.0786	113	-	0.1772	12.8861	2.0788
2.0127	-	-	-	-	-
1.7354	024	-	0.2364	12.9361	1.7355
1.5988	116	-	0.1772	12.9701	1.5988
1.5522	211	-	0.4137	27.7350	-
1.5087	018	-	0.0509	12.9725	1.5087
1.4257	124	-	0.4137	14.3039	1.4258
1.4029	124	-	0.4137	13.0188	1.4028
1.3721	030	4.7534	0.5316	-	-
1.2346	119	-	0.1772	13.0066	1.2346
1.1884	220	4.7518	0.7092	-	-
1.1456	223	-	0.7092	13.0558	1.1455
1.1231	128	-	0.4137	12.9931	1.1233
1.0970	0.2.10	-	0.2364	12.9695	1.0970
1.0780	134	-	0.7682	13.1661	1.0780
1.0431	226	-	0.7092	13.0960	1.0430
0.9982	1.2.10	-	0.4137	13.0199	0.9982

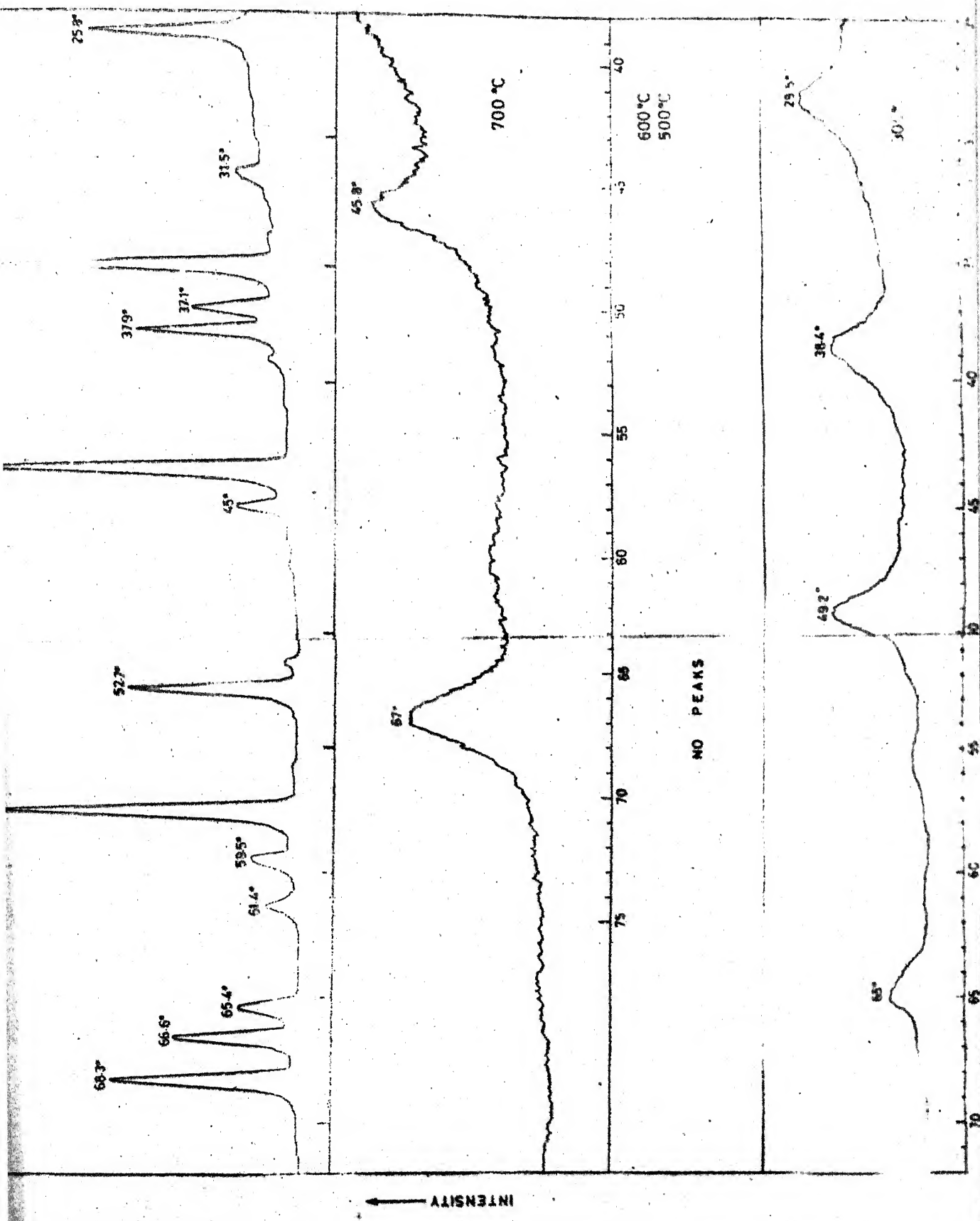

ig. 2.3 Effect of firing temp. on crystallinity.

3. When amorphous alumina is further heated to 800°C, it starts crystallizing. A very few diffraction peaks were observed in this sample which matched to chi-, eta- and gamma-forms of alumina. Number of diffraction peaks increase with the firing temperature and till 1000°C, they correspond to Chi-, eta- and gamma alumina.

On heating at 1000°C, the mixture of chi-, eta- and gamma alumina transforms to alpha alumina and it completes at 1300°C.

The lattice parameters for α-alumina determined are a=b= and c=

(b) DTG, DTA & TG studies

When aluminium hydroxide is heated from room temperature to successively higher temperatures, several type of chemical and structural transformations associated with heat evolution (exothermic) or heat absorption (endothermic) take place. As all these transformations do not occur at the same temperature, a record of local temperature and weight of sample with heating temperature help in recognising the specific process of thermally activated transformation. Most important of these in the present situation are desorption of external water, dissociation of aluminium hydroxide, amorphous to crystalline transitions and transformation from one crystalline form to other in alumina. Thus, dried aluminium hydroxides (fired at various temperatures) were studied using DTG, DTA & TG techniques. The derivatograph

used, is shown in Fig. 2.4.

The samples were heated in ambient atmosphere from room temperature to 1000°C with a heating rate of 10°C per minute and various plots were recorded on photographic paper mounted on a cylindrical drum. Differential Thermal Analysis (DTA) curve records heat evolution (or absorption) effects associated with phase changes or chemical reactions of the sample. In Thermogravimetry (TG) curve the weight of sample is recorded continuously and the course of the reaction is followed through measuring weight changes. Derivative Thermogravimetry (DTG) is a record of the rate of change of weight loss and gives a measure of reaction rate of various temperatures. These records (curves) for various samples are shown in Fig. 2.5 (a,b,c,d).

Each of the sample, fired at 50°C and 200°C, exhibits endothermic DTA peaks followed by DTG peaks within 10 to 20°C. These correspond to loss of weight due to dehydration of hydrated aluminium-hydroxide. The weight loss in the first case is 6.92% at 120°C and 10.8% at 150°C. As none of these weight loss correspond to dehydration of aluminium hydroxide they are attributed to loss of external water. The next DTA peaks appear at 320° for the 50°C-fired sample and 340° for 200°C-fired sample. The corresponding water loss is about 15% in both the cases. The percentage of water loss due to dehydration of pure AlOOH is about 19.5% for Boehmite form.

It is therefore thought that second DTA (DTG) peak appear due to dehydration of Boehmite form. Existence of this form has been confirmed by X-ray analysis. The hydroxide in the present investigation may be a mixture of crystalline Boehmite (predominant) and amorphous trihydroxides. Thus, the third peak in these two samples (i.e. 520°C in the first and 540°C in the second) may be due to dehydration of amorphous alumina trihydroxides. The sample, fired at 600°C, does not show peaks due to dehydration and water loss (maximum around 10%) results continuously with rise of temperature. 1000°C-fired sample shows no peaks in DTG or DTA, as it was expected.

It is difficult to explain the presence of some exothermic peaks in the present case and also more weight loss in the case of 200°C-fired sample.

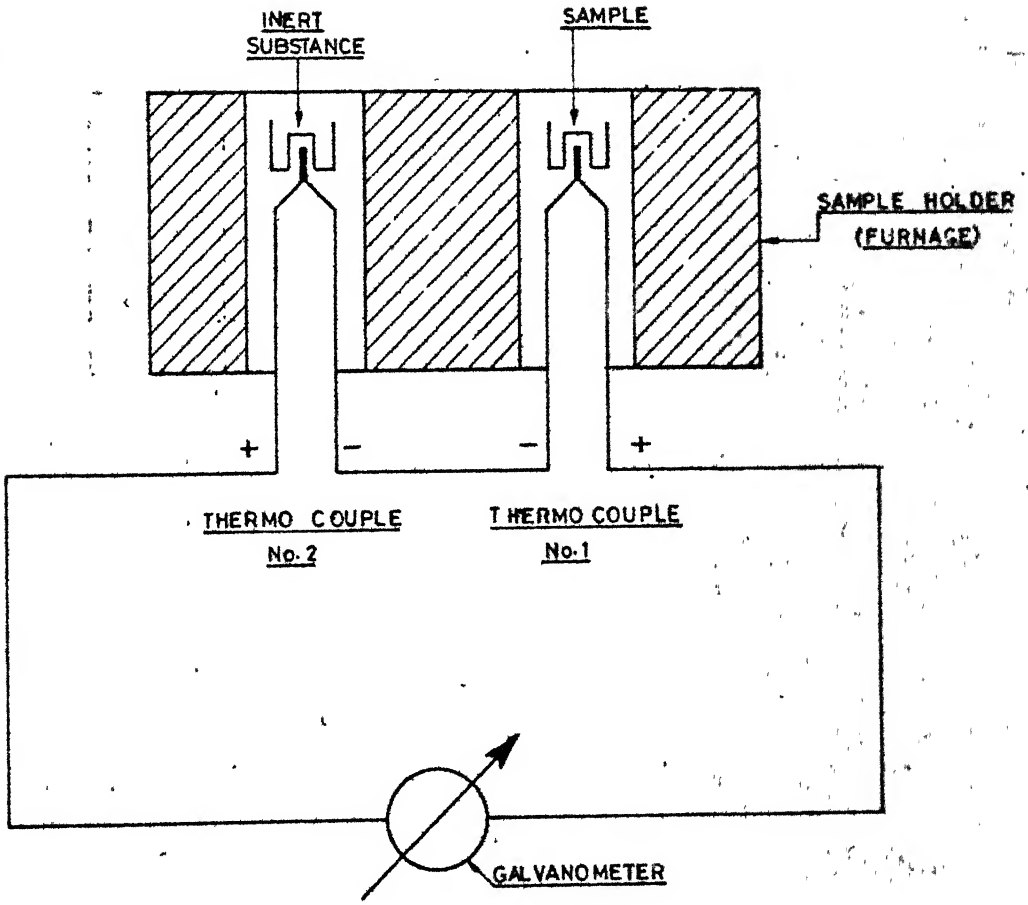

Fig. 2.4 LINE SKETCH OF DERIVATOGRAPH

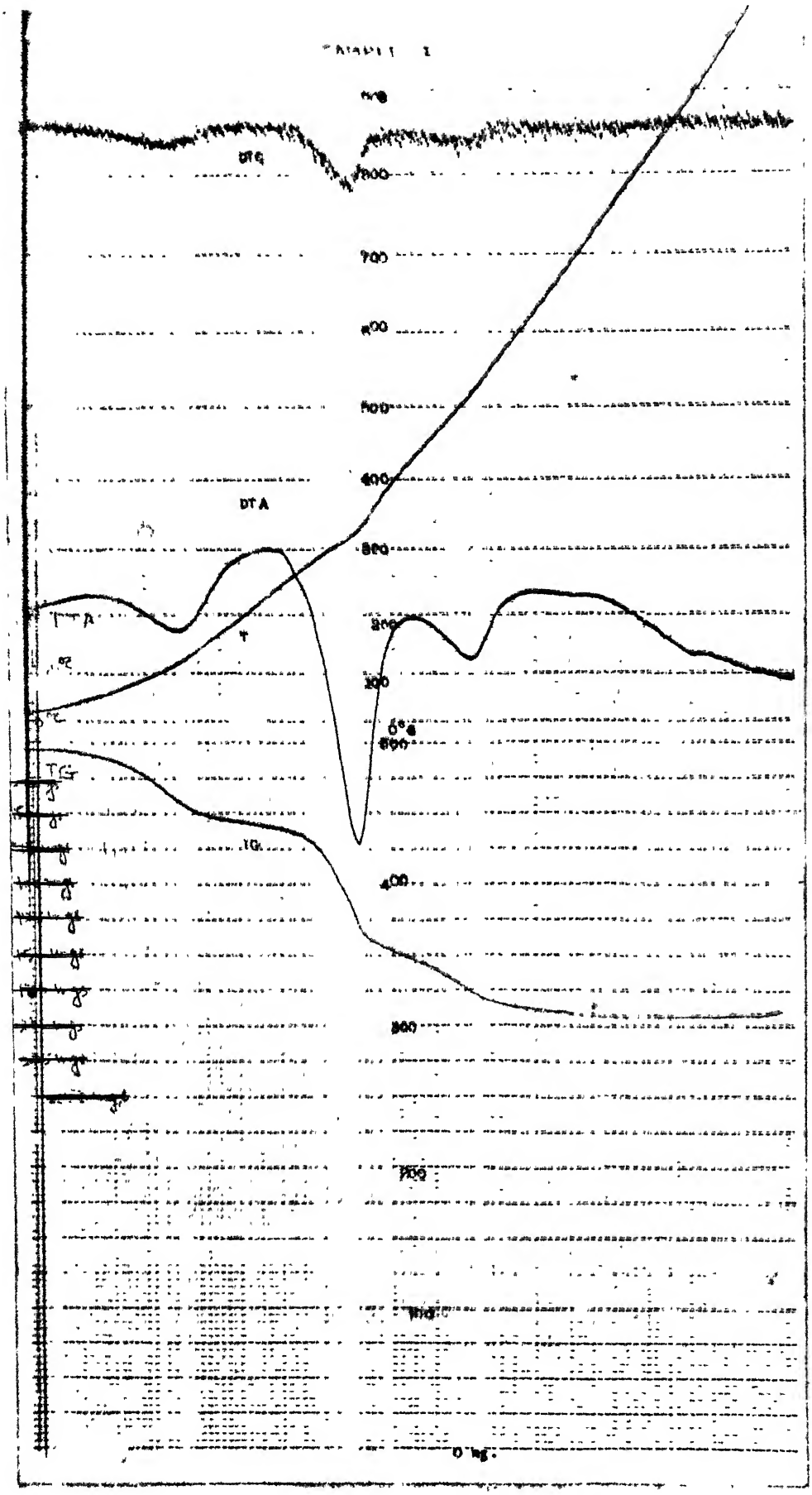

Fig. 2.5(a) DTG, DTA & TG of alumina, fired at 50°C

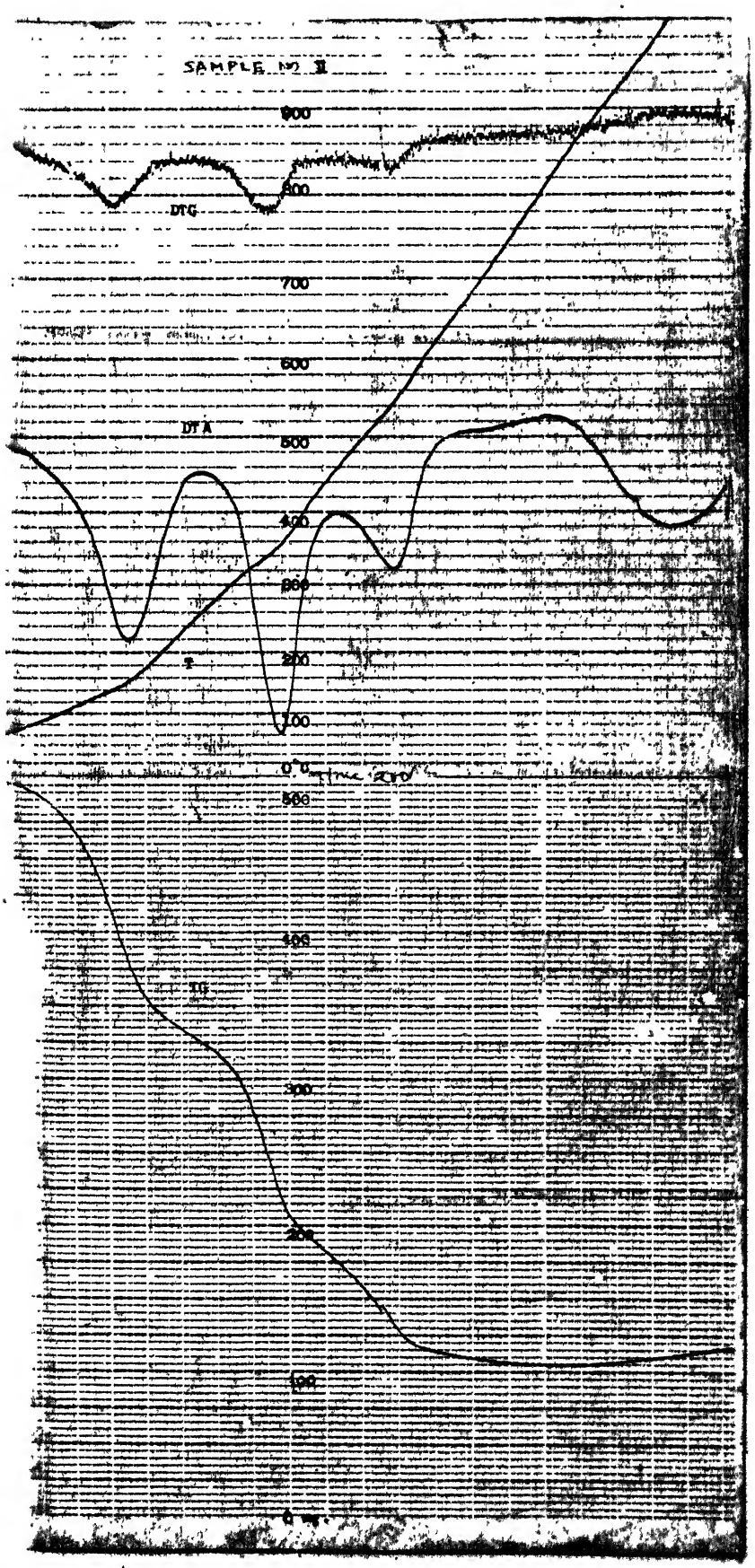

Fig. 2.5(b) DTG, DTA & TG of alumina, fired at 200°C

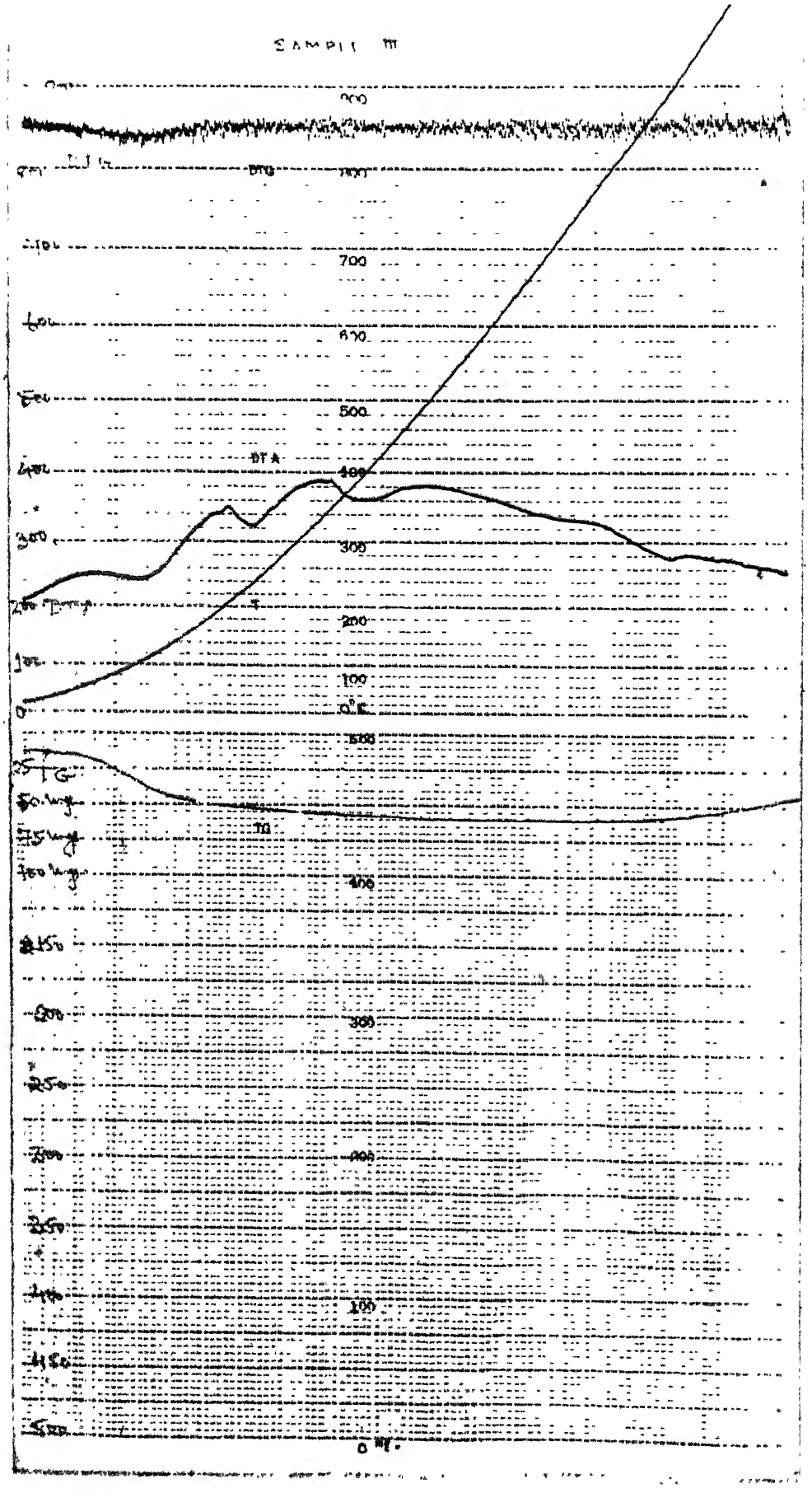

Fig. 2.5(c) DTG, DTA & TG of alumina, fired at 600°C

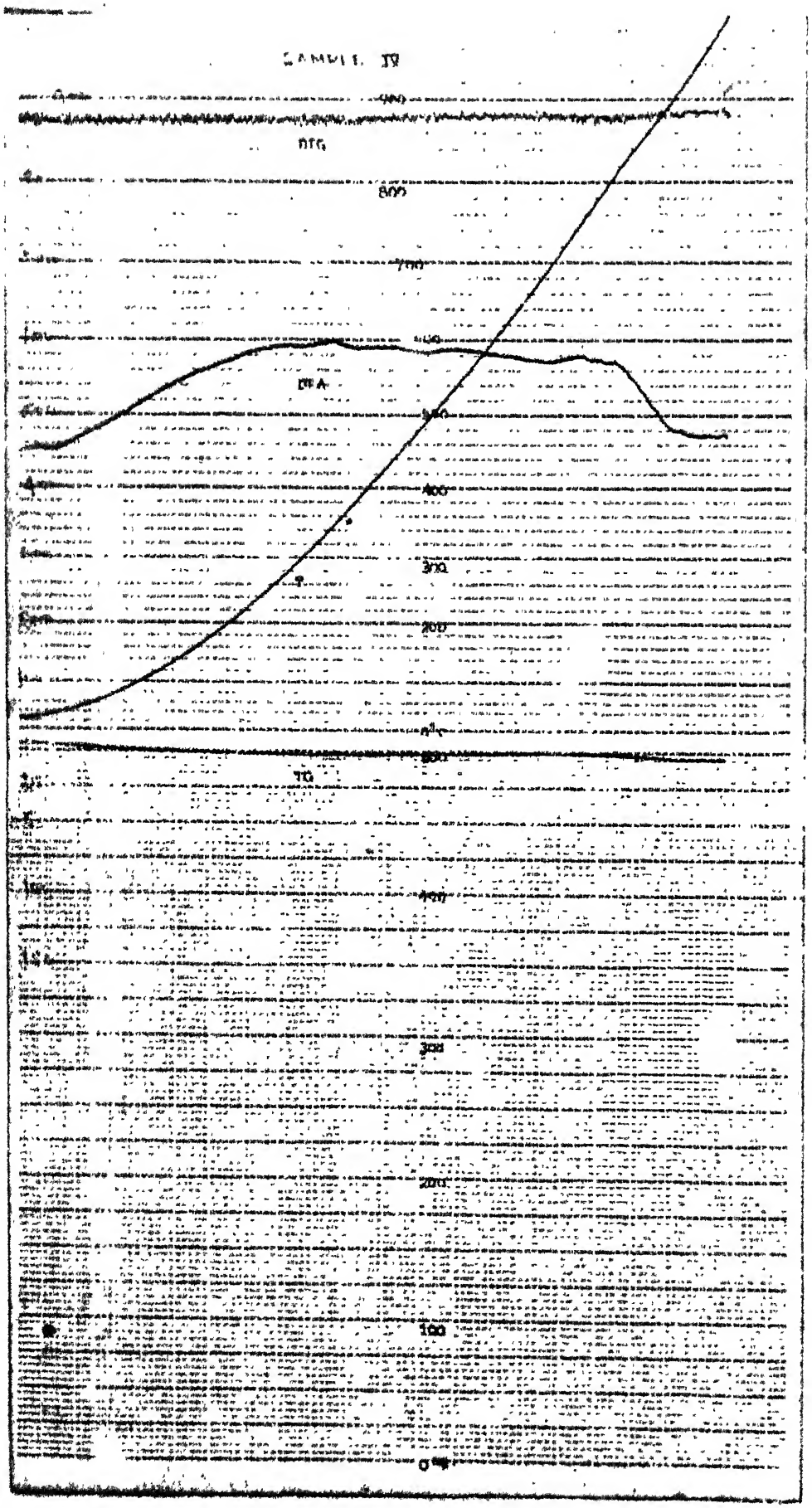

Fig. 2.5(d) DTG, DTA & TG of alumina, fired at 1000°C

Table 2.6 DTA, DTG & TG Studies

(temp. in °C and weight in mgs.)

	Sample fired at 50°C		Sample fired at 200°C		Sample fired at 600°C		Sample fired at 1000°C	
	Peak temp.	%Weight loss	Peak temp.	% Weight loss	Peak temp.	%Weight loss	Peak temp.	%Weight loss
DTG	110	5.79	160	9.13				
	320	20.66	340	23.91				
	520	29.75	540	37.17				
	(Endothermic)		(Endothermic)		No peaks		No peaks	
DTA	120	6.92	150	10.87	200	8.77		
	330	21.49	360	24.78	340	9.65		
	520	29.75	550	37.17			No peaks	
	(Endothermic)		(Endothermic)		(Exothermic)			
Maxm. % Weight loss	32.23		34.35		10.53		0.56	

(c) Electron Microscopic Studies

Electron microscopy is a powerful tool in the characterization of ultrafine ceramic powders. In the present work particle size distribution and shape characteristics of Hydrolysed Aluminium isopropoxide (Al-hydroxide) and calcined product have been studied. d-values also have been calculated and compared with those of standard.

Saturated solution of aluminium isopropoxide in Isopropyl alcohol was prepared and its one drop was added in 15 c.c. of distilled water resulting in the formation of aluminium hydroxide. After dispersion of hydroxide, a drop of it was kept on a carbon coated grit (200 mesh). After drying the support grit, it was injected in the microscopic column (Phillips EM 301 Transmission Electron Microscope). The microscopic study was carried out at resolution of 10 A°. Standard Gold diffraction pattern was first photographed for determining the camera constt. (cm.A° at 100 Kv)

The first electron micrograph Figure-2.7(b) shows needle shaped particles of hydrolyzed Aluminium isopropoxide (Al-hydroxide). The electron diffraction pattern, obtained from this, is shown in Figure 2.7(a). d-values for this sample have been calculated (Table 2.7) which correspond to boehmite. When these particles were heated by electron beam, they disintegrate into smaller particles. Figure 2.8(b) Though the temperature due to electron beam heating could not

Fig. 2.6 Electron diffraction pattern of Gold.

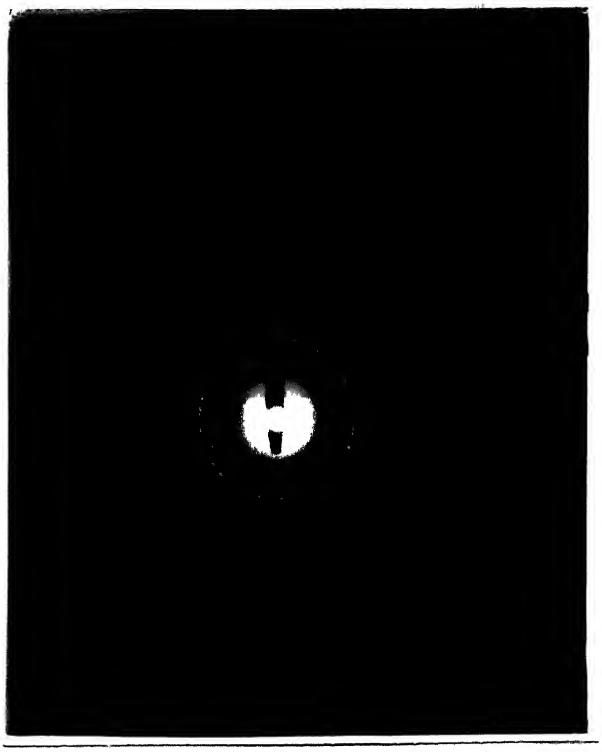

Fig. 2.7(a) Electron diffraction pattern of aluminium hydroxide.

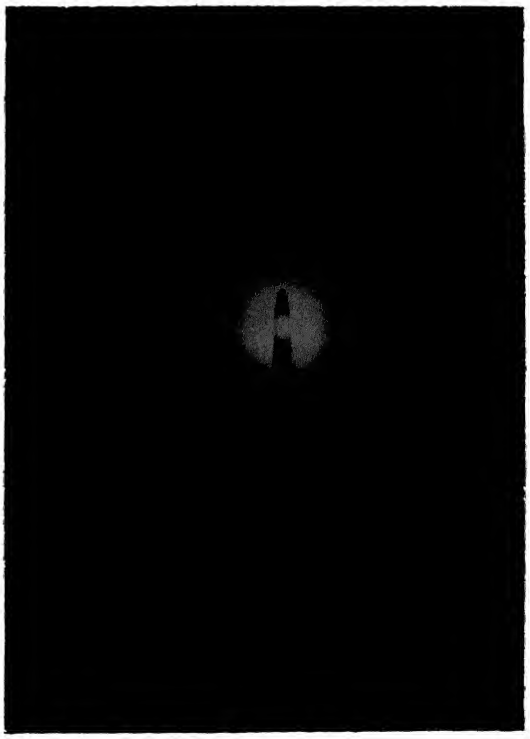

Fig. 2.8(a) Electron diffraction pattern of amorphous alumina.

be determined. It is estimated to be below 800°C, because it produced amorphous alumina as evidenced by electron diffraction pattern Fig. 2.8(a) .

The average particle size of amorphous alumina, as determined from frequency distribution of electron beam heated alumina is

2(D)

SINTERING BEHAVIOUR

Synthesized powders were calcined at 500°C for 6 hours to transform Aluminium hydroxide into amorphous alumina. It was further ground to -200 mesh size as during calcination materials turn out to be lumps. Later on, this powder was pelletized for sintering studies.

(a) Pelletization

The above powder was further pressed into cylindrical pellets of thickness between 0.52-0.56 cm. in a 1.30 cm. diameter split die. A pressure of 10 Tons was applied through a hydraulic press (Carver Lab. Press. Model M) each time.

(b) Sintering

Sintering was carried out in a Globar furnace. Heating rate was approx. 200°C/hour, while cooling rate was much faster i.e. approx. 300°C/hour. Sintering was conducted at 1000°C, 1100°C, 1200°C, 1300°C and 1400°C for a period of 6 hours in each case. The temperature was maintained to an accuracy $\pm$ 5°C.

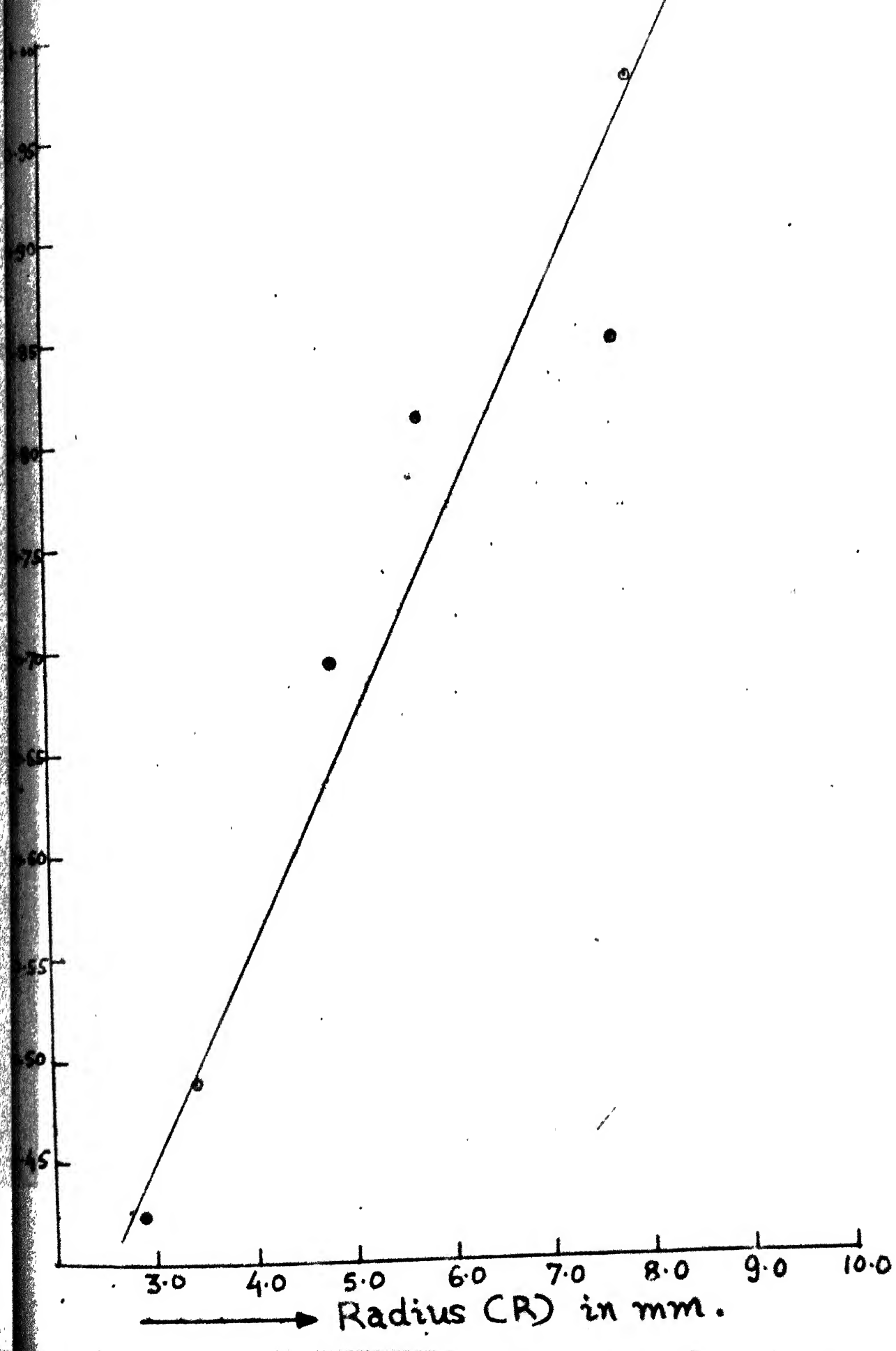
95
90
85
80
75
70
65
60
55
50
45
3·0
4·0
5·0
6·0
7·0
8·0
9·0
10·0
Radius (R) in mm.

Table 2.7

Calculation of d-values for Aluminium hydroxide sample

Electron diffraction pattern of Gold

d_{hkl}	$1/d_{hkl}$	Radii of rings (R in mm.
2.355	0.4246	2.9
2.039	0.4904	3.4
1.442	0.6935	4.8
1.230	0.8130	5.7
1.177	0.8500	7.7
1.020	0.9804	7.9

($1/d_{hkl}$ is plotted against R in Fig. 2.8(c) to get standard curve)

Electron diffraction pattern of Al-hydroxide

Radii of rings (R) in mm.	$1/d_{hkl}$ (from Fig. 2.8c)	d_{hkl}
2.5	-	-
2.7	0.4175	2.3952
3.8	0.4475	2.2346
4.7	0.5325	1.8779
5.5	0.6275	1.5936
5.7	0.7125	1.4035
6.2	0.7325	1.3651
7.1	0.8800	1.1364
7.6	0.9400	1.0638
8.0	0.9825	1.0178

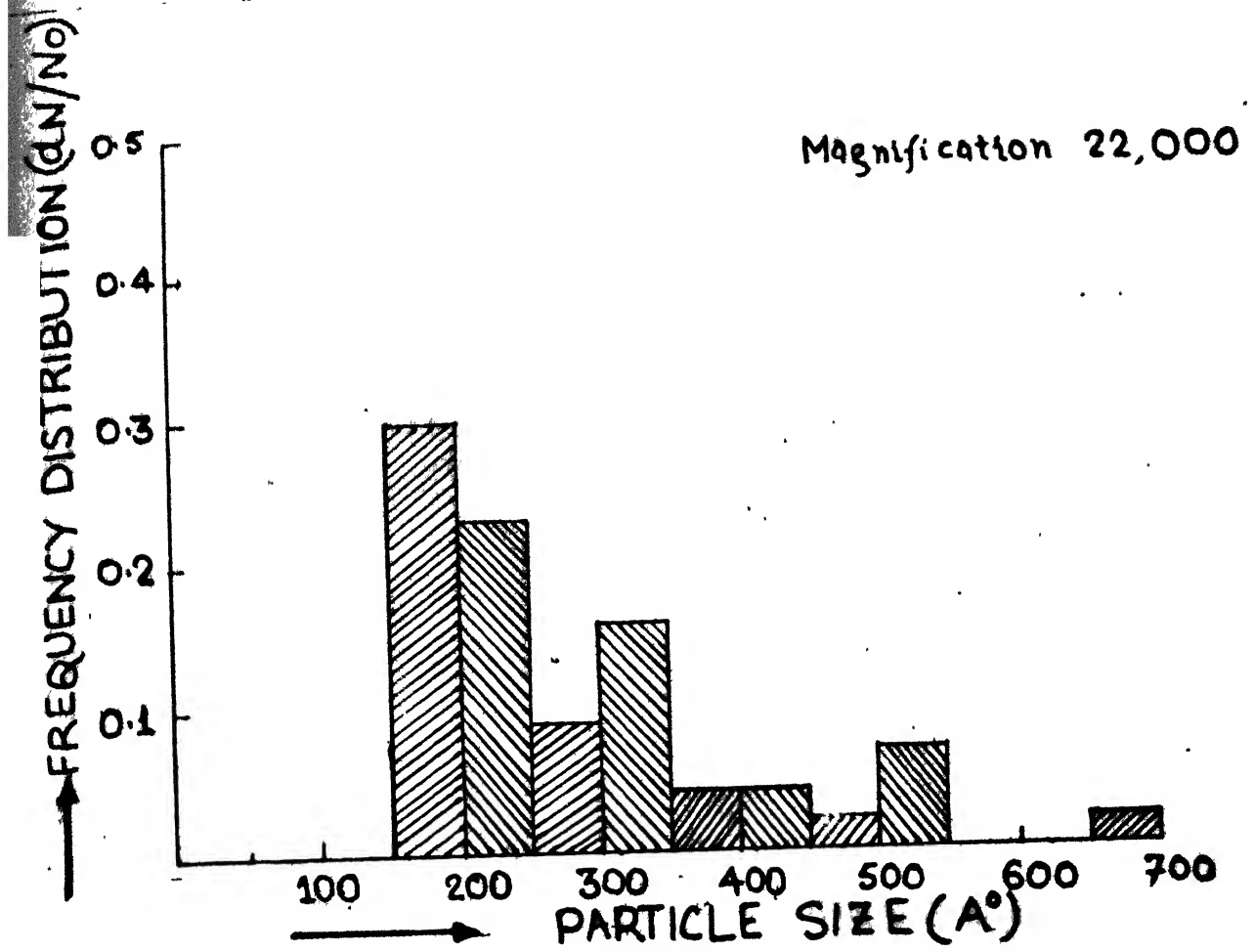
Magnification 22,000
FREQUENCY DISTRIBUTION (dN/No)
0·5
0·4
0·3
0·2
0·1
100
200
300
400
500
600
700
PARTICLE SIZE (A°)

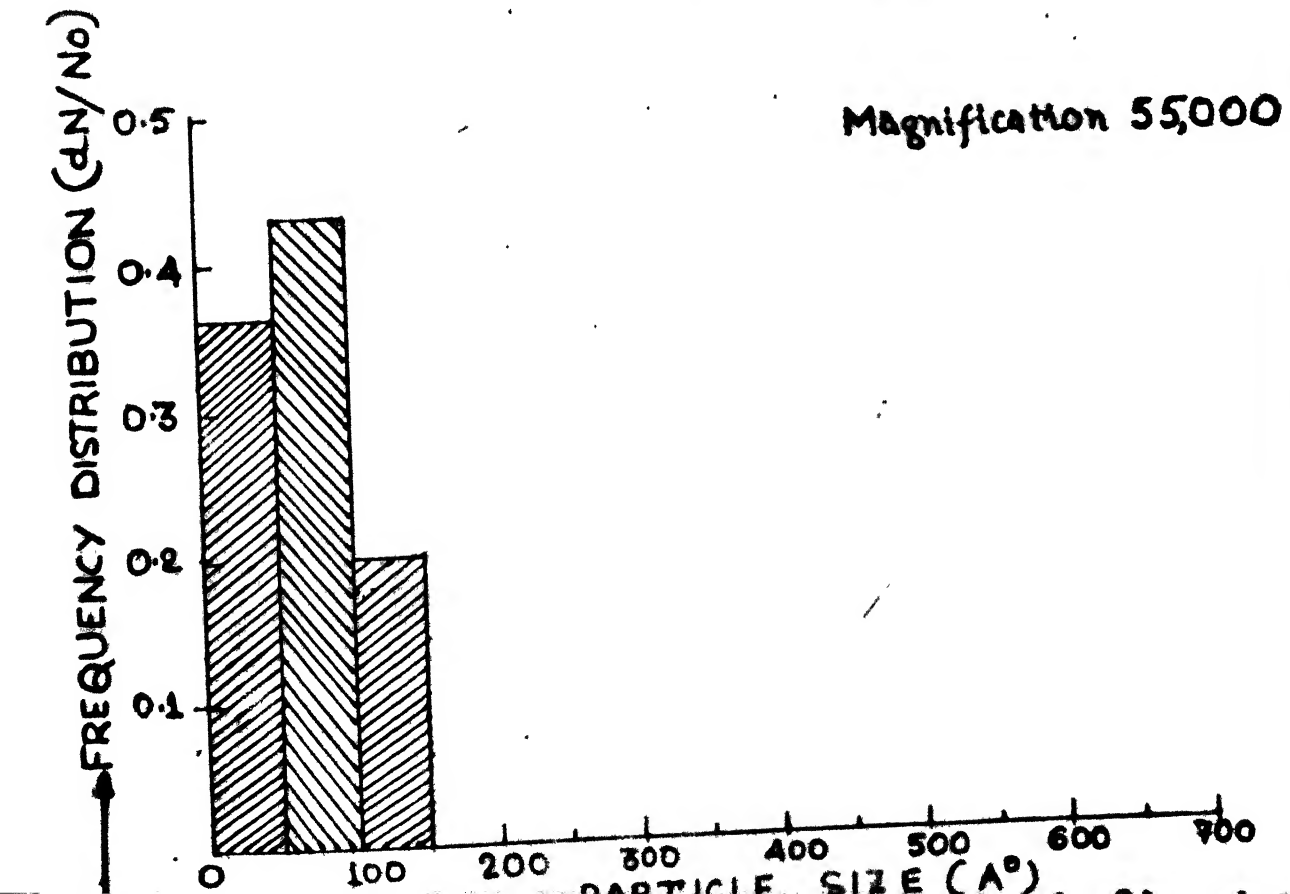
Magnification 55,000
FREQUENCY DISTRIBUTION (dN/No)
0·5
0·4
0·3
0·2
0·1
0
100
200
300
400
500
600
700
PARTICLE SIZE (A°)

Table 2.8 Density of fired Alumina pellets

Firing temp. (in kelvin) T	$\frac{1}{T}$ x 1000	Density (gm/ml.) Before firing	Density (gm/ml.) After firing	Density change	log ρ
1273	0.785	1.5186	1.6212	0.1026	- 0.988
1273	0.785	1.4924	1.6379	0.1455	- 0.837
1373	0.728	1.5191	1.8302	0.3111	- 0.507
1373	0.728	1.4890	1.7200	0.2310	- 0.636
1473	0.679	1.5396	2.0459	0.5063	- 0.295
1473	0.679	1.5043	1.9401	0.4358	- 0.360
1573	0.636	1.5169	1.9369	0.4200	- 0.376
1573	0.636	1.4890	2.0184	0.5294	- 0.276
1673	0.598	1.5245	2.2461	0.7216	- 0.141
1673	0.598	1.5292	2.3361	0.8069	- 0.093

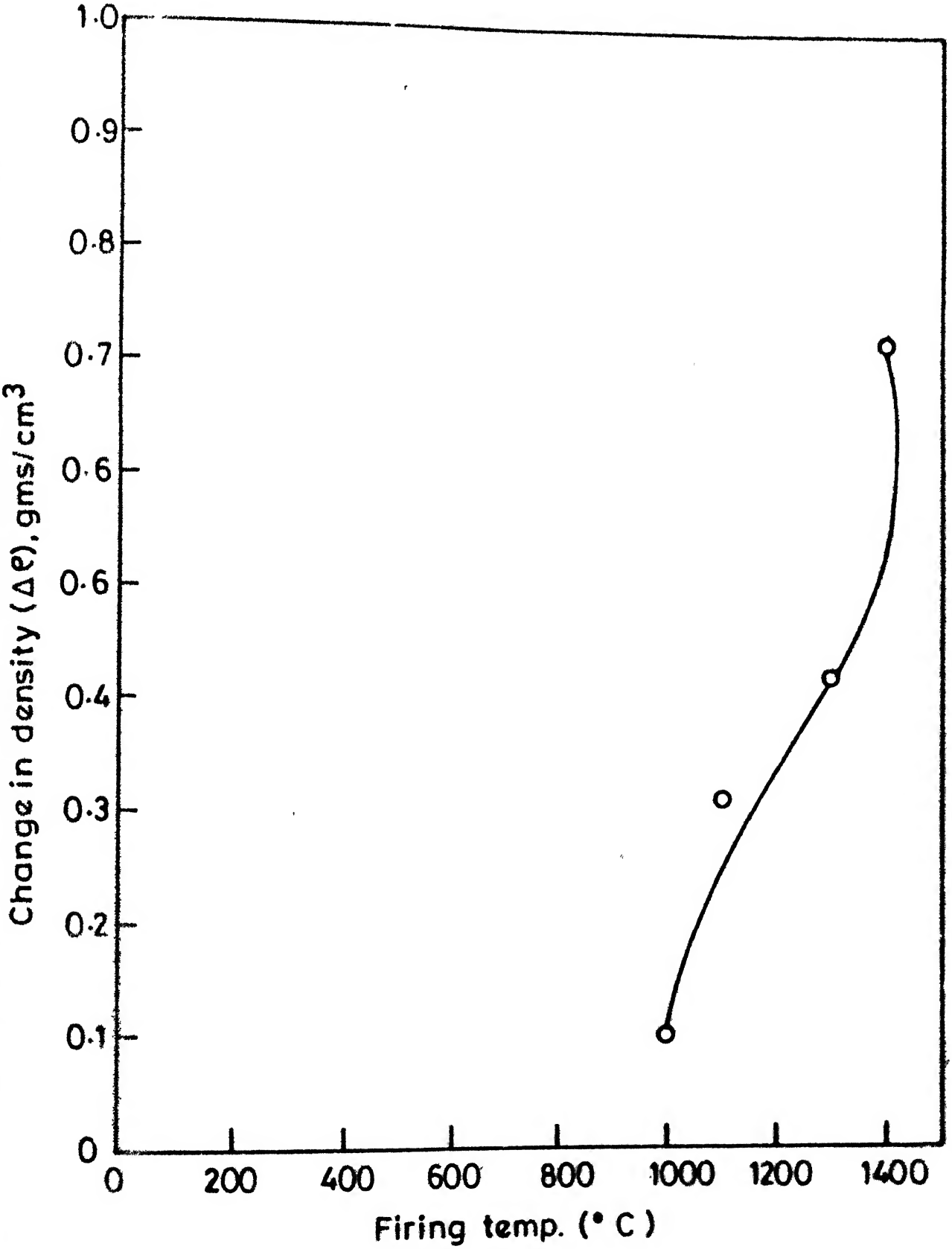

Fig. 2.10 Effect of firing temp. on density-change.

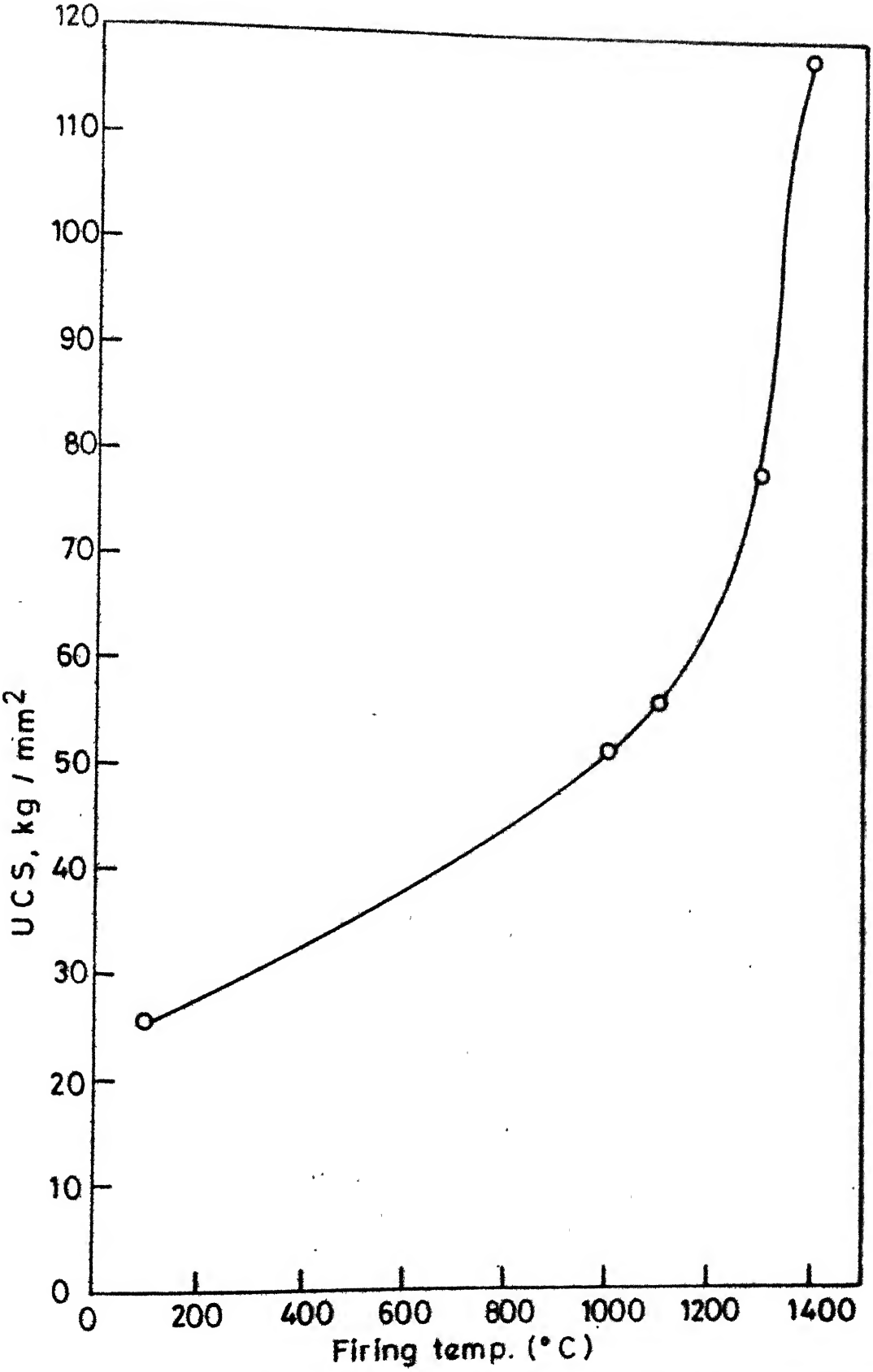

Fig. 2.11 Effect of firing temp. on ultimate compressive stress.

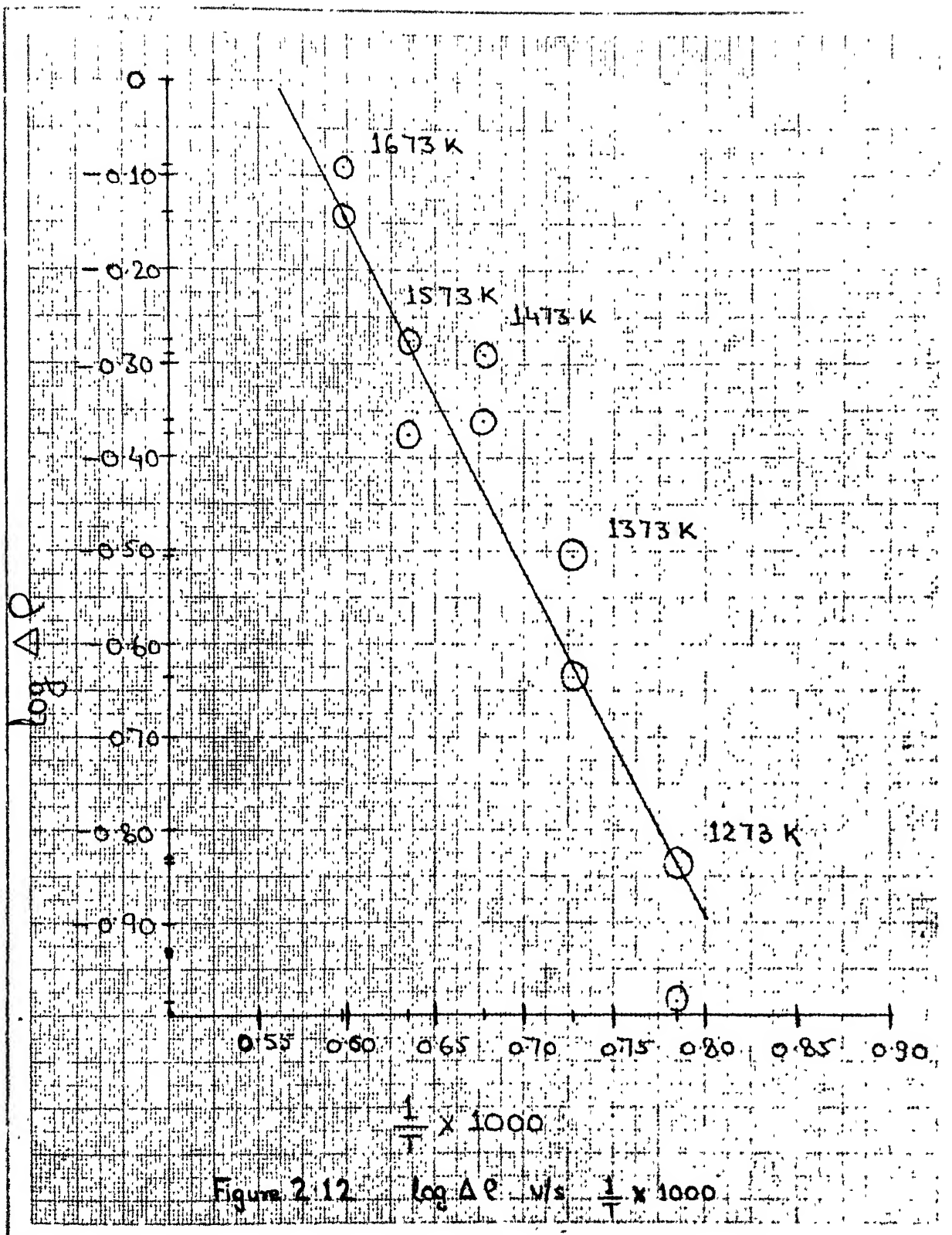

Figure 2.12 $\log \Delta \ell$ v/s $\frac{1}{T} \times 1000$

(c) Density measurements

All the green and fired pellets were weighed and their diameter and thickness were measured for density measurements. From these data, the change in density on sintering were calculated. (Table 2.8)

(d) Sintering Kinetics

The rate of change in the density seems to increase with sintering temperature as

$$\frac{d\rho}{dt} = A.e^{-\Delta E/RT}$$

Thus Arrhenius plot between $\frac{d\rho}{dt}$ and $\frac{1}{T}$ gives straight line as shown in Figure 2.12. The activation energy and pre-exponential term were found to be 16.84 K cal./mole and sec^{-1} respectively.

(e) Fracture strength with sintering

Compressive strength of each of the pellets were determined using Instron. The results are tabulated as follows.

Table 2.9 Ultimate Compressive Strength of Pellets

Firing temp. (°C)	Pellet area of cross section (mm^2)	Load (Kg.)	Ultimate Compressive Stress (Kg/mm^2)
Unfired	133.60	1150	8.60
1000	120.81	2000	16.55
1100	110.50	2100	19.00
1300	105.72	2850	26.95
1400	94.72	4100	43.28

REFERENCES

1. Karl Wefers and Gordon M. Bell, "Oxides and Hydroxides of Aluminum", technical paper No. 19, Alcoa Research Laboratories, 1972.

2. D.F. Saunders et al, "Effects of rate and temperature of mixing on the surface area of precipitated alumina hydrates", Chem. Ind. (London), 18, 594, 1970.

3. R.E. Jaeger et al, "Preparation of ceramic oxide powders by liquid drying", Am. Ceram. Soc. Bull, 53, (12), 854, 1974.

4. W.S. Claubaugh, E.M. Swiggard, R. Gilchrist, Vol. 56, p. 289, 1956.

5. Yoldas, J. Mat. Sci. 12, p. 1203, 1977.

6. Torkar and Egghart, Monatsh. Chem. 92, 755-67 (1961).

7. Watson et al, Kolloid-Z. 140, 102-112 (1955); 154, 4-15 (1957).

8. Turkevich and Hiller, Anal. Chem. 21, 475-85 (1949).

9. Teichner, C.R. Acad. Sci. 237, 810-2, 900-2 (1953).

10. Papee et al, Bull. Soc. Chim. Fr. 1301-10 (1958).

11. Harris and Sing, J. Appl. Chem. 5, 223 (1955); 7, 397 (1957); 8, 386-9 (1958).

12. Hsu and Bates, Contrib. No. 62-50, Coll. Miner. Ind., P. State Univ. (1962).

13. Pavella, Kolloid-Z. 107, 139-41 (1944).

14. Schmah, Z. Naturforscher. 1, 323-4 (1946).

15. Bugosh, U.S. Patent 2915475 (Dec. 1, 1959).

16. Millgan and Weiser, J. Phys. Colloid Chem. 55, 490-6 (1951).

17. Fricke and Wullhorst, Z. Anorg. Allg. Chem. 205, 127-44 (1932).

18. Fricke and Jockers, Z. Naturforsch. 2b, 244 (1947).

19. Torkar and Bergmann, Monatsh. Chem. 91, 400-5 (1960).

20. Schmah, Z. Naturforscher, 1, 323-4 (1946).

Chapter 3

PREPARATION & CHARACTERIZATION OF ACRYLIC ACID POLYMER

Abstract

Polymerization of acrylic acid monomer has been carried out in aqueous medium using benzoyl chloride as an initiator. The molecular weights of these polymer samples as a function of processing conditions have been investigated.

3(A)

INTRODUCTION

Acrylics are the derivatives of acrylic acid (CH_2 = CHCOOH) and methacrylic acid, CH_2 = $C(CH_3)$COOH. They have acquired industrial significance due to their useful properties. Important applications of these materials include plastic sheets and moulding powder for signs, construction units and decorative emblems and insignia, polymer solutions for coating application, leather finishing, paper coating and a variety of polymers for sizing, treating and finishing textiles. Derivatives of acrylic acid and methacrylic acid, together are used in many applications to achieve desired properties.

Some physical properties of acrylic acid monomer are displayed in the Table 3.1.

Table 3.1

m.p.	13.5°C
b.p.	141°C
density	1.045 gm./ml.
Refractive Index	1.485 (25°C)
Kinetmatic Viscosity	1.1 (25°C)
Dissociation Constant	5.50×10^{-5}
Solubility (in water and organic solvents)	$>$ 5 gms./100 gm. solvent

3(B)

PREPARATION OF POLYMER

Polymerization of acrylic acid is considered an important process. In the present work, the objective of the preparation of polymer is to use it as an dispersent, activator, and binder in the electrophoretic bath for coating alumina.

The polymerization is an exothermic reaction, which needs an initiator. Whatever the initiating species are, the heat liberated by the polymerization of each monomer is a definite and measurable value, called the heat of polymerization (approximately 18.5 cal. for acrylic acid). This heat may be allowed to dissipate slowly by controlling the rate of polymerization or the polymerization may be carried out in a medium that will remove this heat without permitting a violent or dangerous reaction.

Linear polymers of acrylic and methacrylic acids may be synthesized by the general methods as used for vinyl monomers e.g. using suitable initiators. The chemical reaction, involved, is as follows:

$$n\ CH_2 = CHCOOH \xrightarrow[\text{Energy}]{\text{Initiator}} m - CH_2-\underset{\underset{COOH}{|}}{CH} - CH_2 - \underset{\underset{COOH}{|}}{CH} - m$$

Acrylic acid is readily polymerized by exposure to visible or ultraviolet light. Polymerization by visible light is hastened if a sensitizer such as boflavin is dissolved in the acid [1] . Acrylic acid has been polymerized by ultraviolet light when in the form of crystals [2]. Crystalline salt of acrylic acid has also been polymerized in a vibratory disintegrator [3] .

Polymerization in aqueous/non-aqueous medium

Polymerization can be carried out either in aqueous or organic media like benzene.

Organic solvents dissolve only monomer. Inititiation is accomplished with initiators such as benzoyl peroxide or azo-bis-isobutyro nitrite soluble in the medium used. In benzene, polymerization can be carried out as a continuous process in which monomer, initiator and solvent are continuously added and a slurry containing polymer and unreacted ingradients is continuously removed. The product of this preparation is a free flowing powder with a density of 0.4 gm./cc.

Polymer solutions in organic solvents, such as methanol and dioxane, may be prepared by the use of azo-bis-isobutylnitrile initiator at elevated temperatures. A solution of acrylic acid may be polymerized with an initiator such as benzoyl peroxide, which may be removed from the reaction medium by filtration.

Present Work

In the present work, acrylic acid was polymerized in aqueous medium. Because of the case of polymerization of diluted solutions of monomer, acrylic acid was taken in different concentrations. These solutions were heated upto 85°C for different durations of time in the presence of benzoyl peroxide as initiator. Benzoyl peroxide was taken in fraction of grams ($\simeq$ 300 mg).

3(C)

CHARACTERISATION OF POLYMER

The variation in the molecular weight of polymer as a function of monomer concentration in water, and duration of heating was investigated. The conditions are given in the Table 3.2. A liquid chromatograph (Water Associates 440 Model) was used for this purpose. The details of instrument were as follows:

Columns	-	¼" - styragel 10^4, 10^3, 500 and 100 A° in series
Solvent	-	THF
Flow rate	-	1.0 ml. per minute
Calibration	-	polystyrene standards, supplied by Water Associates.

Sample No. 3 was used for coating purpose (Ref. Chapter 4).

Table 3.2

Sample No.	Monomer:Water	Duration of heating (minutes)	Molecular Weight
1	1 : 1	10	3.128×10^5
2	1 : 2.5	10	2.2979×10^5
3	1 : 5.0	10	9.2185×10^6
4	1 : 7.5	10	2.9691×10^5
5	1 : 10	10	7.5679×10^5
6.	1 : 5	0	2.2500×10^4
7.	1 : 5	5	8.00137×10^6
8.	1 : 5	10	7.38993×10^6
9.	1 : 5	15	8.34314×10^6

REFERENCES

1. Encyclopedia of Polymer Science and Technology, Vol. I, p. 203.

2. Encyclopedia of Chemical Technology, Vol. I, p. 285-311.

3. C.F. Horn et al, J. Appl. Polymer Sci., 7, 887 (1963).

4. W.R. Sorensen et al, Preparative methods of polymer chemistry, Interscience Publishers, Inc., N.Y., p. 129.

5. J.R. Schaefgen et al, J. Polymer Sci., 40, 377 (1959).

Chapter 4

ELECTROPHORETIC DEPOSITION OF ALUMINA

Abstract

Alumina (A.R. grade) and synthesized amorphous alumina have been coated on stainless steel and graphite plates through Electrophoretic deposition using acrylic acid-polymer, prepared in laboratory. The coatings, later on, have been fired at 1600°C in Argon atmosphere.

4(A)

INTRODUCTION AND LITERATURE REVIEW

The phenomenon of electrophoresis is the movement of colloidal particles, suspended in an aqueous or non-aqueous medium under an electrical field. This property was first observed by a Russian physicst Reuss and has been used for the deposition of metals, their oxides and in separation of protiens from blood plasma.

Recently electrophoretic deposition from aqueous and organic media has got great technological importance. Fahnoe et al [1] coated fine Al_2O_3 and NiO particles from thick suspension of isopropyl alcohol. Deposition of carbonates of Ba-Sr (0.5 - 50 μ particle diameter) through acetone medium using nitrocellulose as binder have been attempted by Benjamin and Osborn [2] .

Barium titanate has been deposited on metal sheets from a mixture of $BaTiO_3$, dielhyl glycol, dimethyl ether and Ketol-60 by Senderof and Reid [3].

Werner and Ride Jr. [4] deposited alloy containing 80% Nickel and 20% Chromium using a suspension of metal and metal oxide powder in isopropyl alcohol, nitromethane and zein solution.

Andrews et al [5] and Powers [6] have worked on the fabrication of ceramic wares through this technique.

In case of electrophoretic deposition from aqueous medium, works of Caley [7], Fisch [8] and Kucharski [9] are quite significant. Caley has investigated the effects of different parameters on the quality and quantity of Al_2O_3, Fe_2O_3, Cr_2O_3, NiO, MnO and TiO_2 coatings. The aqueous medium, used by Caley had polyacrylic acid as dispersant and triethylamine as neutralizing base.

A study on aluminide coatings was done by Fisch [8], using amine-solubilized acrylic resin as a dispersant.

Kucharski [9] has reported successful electrophoretic deposition of thick WO_3 and Cr_2O_3 coatings from an aqueous suspension.

4(B)

THEORY OF ELECTROPHORETIC DEPOSITION

Electrophoretic deposition of substances depend upon the migration of suspended particles in a medium under external electric field. Various theories and models have been put forwarded to explain this migration behaviour of suspended particles. The existence of double layer, affecting migration of colloidal particles was proposed by Helmholtz, Gouy - Chapman and Stern. Their models are being described in following section.

The Electrical Double Layer Theory

The particles of most substances acquire a surface electric charge when brought in contact with a polar medium. As a result, a potential difference at the interface of the particle and that of the fluid is established. This property of surfaces and interfaces explains the 'Electrokinetics' i.e. electrophoresis, electro-osmosis, streaming potential and sedimentation potential of suspended particles. The direction of electrophoretic migrations (known as electrophoresis) and its complement, electro-osmosis, are indicated in Figure 4.1. The picture of electric double layer on a spherical particle is shown in Figure 4.2.

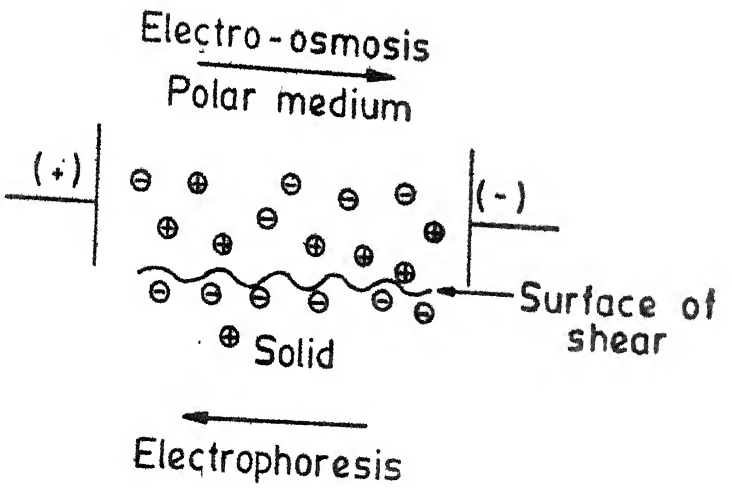

Fig. 4·1– Electrokinetic phenomena.

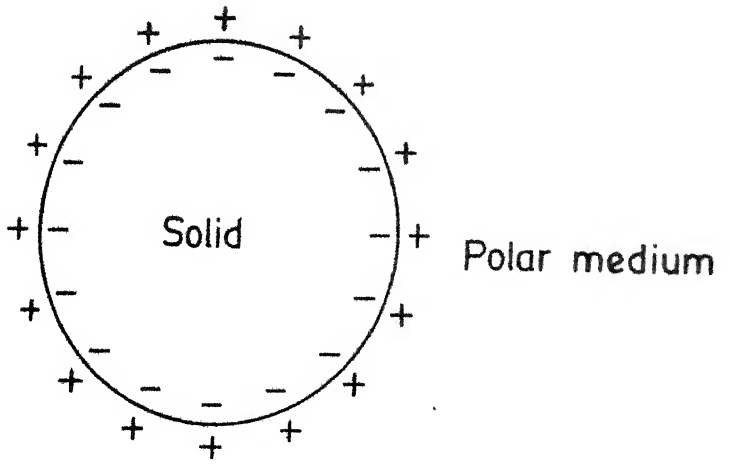

Fig. 4·2–Schematic diagram of electric double layer.

Helmholtz Double Layer

Helmholtz [5,10] introduced a parallel plate condenser model for the electric double layer, which is schematically shown in Figure 4.3. As the particles acquire surface charge in suspension, the oppositely charged particles are attracted towards the surface and in equilibrium, it establishes a double layer. This double layer consists of two oppositely charged planes with charge, σ_s on the solid and σ_L in the solution. This picture of the double layer is analogous to a parallel plate condenser. This leads to the expression :

$$\sigma_s = -\sigma_L = \frac{\varepsilon}{4\pi\delta}\Psi_o$$

Where Ψ_o is the potential across the double layer, ε the appropriate dielectric constant, δ is the distance between the layers. The capacity per unit area, C, of this condenser is then given by

$$C = \frac{\sigma_s}{\Psi_o} = \frac{\varepsilon}{4\pi\delta}$$

This model predicts constant capacity of the double layer determined by the size of ions near the surface and is independent of σ_s, Ψ_o and solution concentration.

Gouy-Chapman Model 12

This model is shown in Figure 4.4. In reality, the ions in a solution diffuse away from the surface because of thermal energy. It predicts the existence of abnormally large counter-ion concentration near the surface and concludes abnormally large value of capicitance at potentials from Point Zero Charge (PZC

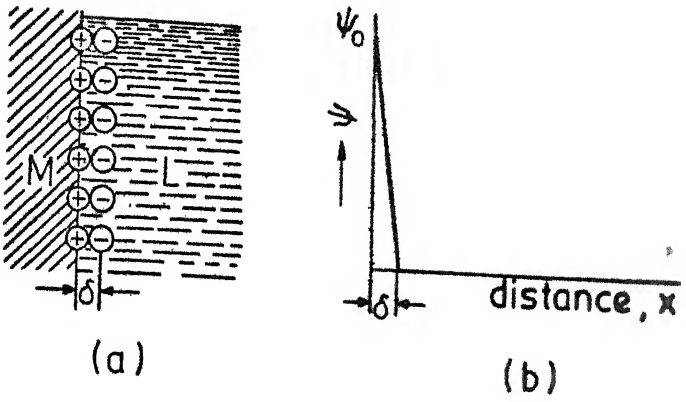

Fig. 4·3 - The Helmholtz model of the double layer : (a) molecular picture; (b) variation of potential with distance from the metal - solution interface.

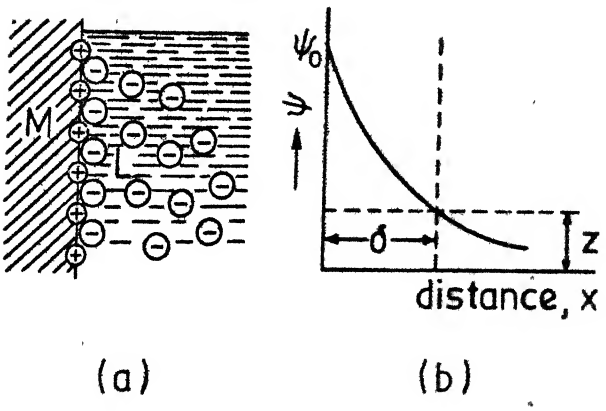

Fig. 4·4 - The Gouy - Chapman diffuse - charge model of the double layer : (a) molecular picture, (b) variation of potential with distance from the metal - solution interface.

Stern Model

In Stern's model [13], double layer is divided into two regions separated by a plane, located about a hydrated ion radius from the surface. The charge distribution on the solution side of the double layer is made up of (i) an ionic layer of charge σ_s lying in a plane parallel to the interface but at a distance δ (of the order of molecular dimension) from it and (ii) the diffuse space charge σ_d of the Gouy - Chapman model.

$$\sigma = - (\sigma_s + \sigma_d)$$

The zeta potential is measured between the surface of shear and the diffuse layer, and thus depends on the nature of the mobile part of the double layer (Figure 4.5).

Stern also indicated the importance of specific adsorption at the interface. Thus, his model, in addition to the smoothed out surface charge and the diffuse space charge, includes a layer of specifically adsorbed ions which may exceed in magnitude of the charge on the surface. As a result, the potential, ψ_o at this layer may have a sign opposite to that of ψ_o (surface potential).

According to this, the inner region of the double layer, not provided in the Gouy-Chapman model may be conceived of as a molecular condenser filled with solvent molecules. The fundamental relations of the diffuse layer will still apply provided ψ_o is substituted by ψ_δ in the equation.

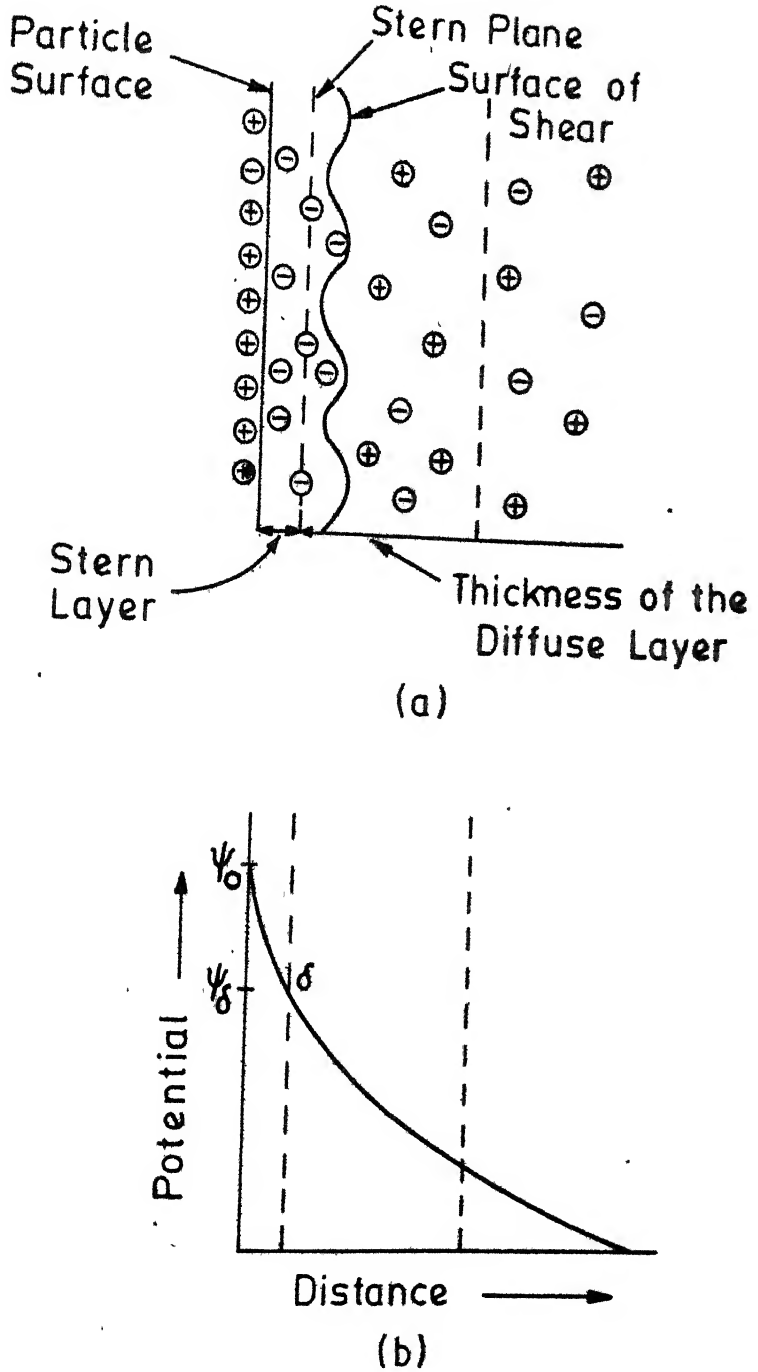

Fig. 4·5 - Schematic representation of electric double layer according to stern's theory:

(a) molecular picture (b) variation of potential with distance from the solid - liquid interface.

The differential capacity C of the double layer is related to C_1, the capacity for inner layer and C_d that for the diffuse layer by the equation,

$$\frac{1}{C} = \frac{1}{C_1} + \frac{1}{C_d}$$

hence, $$C = \frac{d\sigma_s}{d\psi_o} = \frac{d\sigma_s}{d(\psi_o - \psi_\delta) + d\psi_\delta}$$

This is equivalent to a system consisting of two condensers in series. Accordingly, the variation of total capacity 'C' with respect to change $\underset{in}{\sigma_s}$ from pointzerocharge (PZC), would not be very steep because main change is in C_d and not so much in C_1. The predictions from this theory have better fit with the practical conditions.

Further refinement in the theoritical concept has been attempted by some workers [14,10] considering charged particles as point charges. Henry [14,15] , in order to improve the double layer concept further, has included conductivity of the two phases as well.

4(C)

PARAMETERS AFFECTING ELECTROPHORETIC DEPOSITION

During deposition the electrophoretic bath, which comprises of particles suspended in a given liquid (dispersion medium), is of great significance. The pH and solid concentration affect mobility, zetapotential, specific conductivity and viscosity of suspensions. This in turn, influences the quality and quantity of coatings. The suspension medium may be aqueous or organic liquid. Basically, the low viscosity, high density, low electrical conductivity, high dielectric constant, low evaporation rate and good chemical stability are the desired properties of an excellent suspension vehicle (liquid). Low viscosity and high dielectric constant favour a high particle velocity, whereas high density tends to reduce the settling rate. Low electrical conductivity (10^{-4} to 10^{-6} mho/cm^2) is necessary to control the secondary electrode effects (gassing due to electrolysis and heating). Gassing is undesirable since it reduces the coulomb efficiency and damages the deposit. The heating often causes flocculation of the suspension.

A wide study of the effect of different variables has been done in aqueous medium taking various oxides as dispersed phase [16] . For alumina, it was found that specific conductivity increases with pH (Figure 4.6). Further, an increase in percent powder weight concentration (PWC) results in a greater

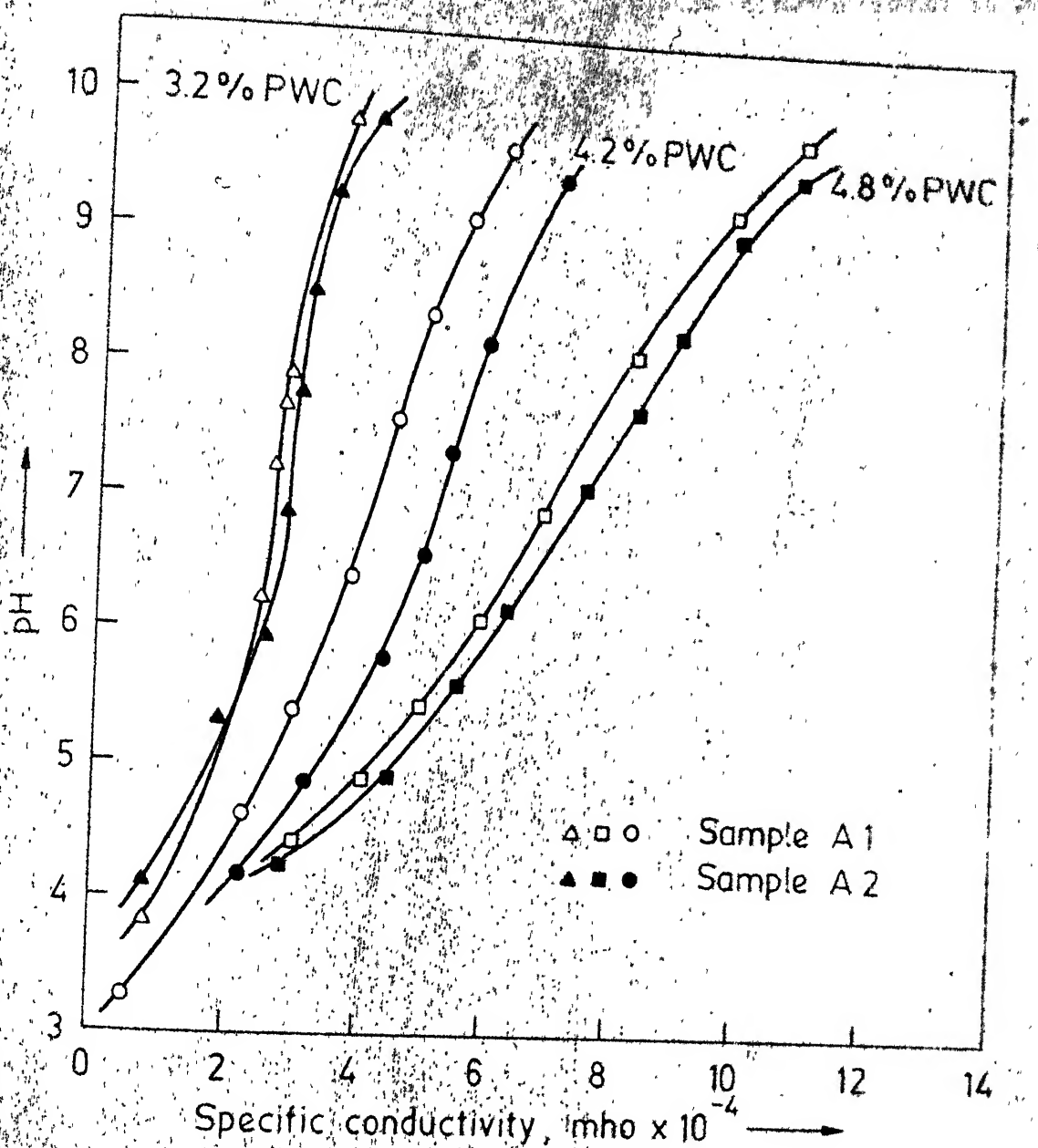

Fig. 4.6 Graph of pH dependence on conductivity for Al_2O_3

conductivity at constant pH. An increase in viscosity with an increase in pH is also apparent for the same PWC (Figure 4.7).

Alumina is stable in acidic as well as in basic medium. It forms a stable suspension at pH lower than 2 and more than 7. The effect of pH on mobility of alumina (A_1 and A_2) has been studied by earlier workers [16] . Their result indicates continuous increase in mobility with pH (Figure 4.7).

The behaviour of pH-mobility and pH-zetapotential profiles depend upon the surface characteristics [16] . The oxides TiO_2, Cr_2O_3, NiO and Fe_2O_3 exhibit similar pH-mobility and pH-zetapotential curves, each approaching a maximum mobility and zetapotential (Figure 4.8 - 4.10). The alumina, however, does not follow this trend (Figure 4.7).

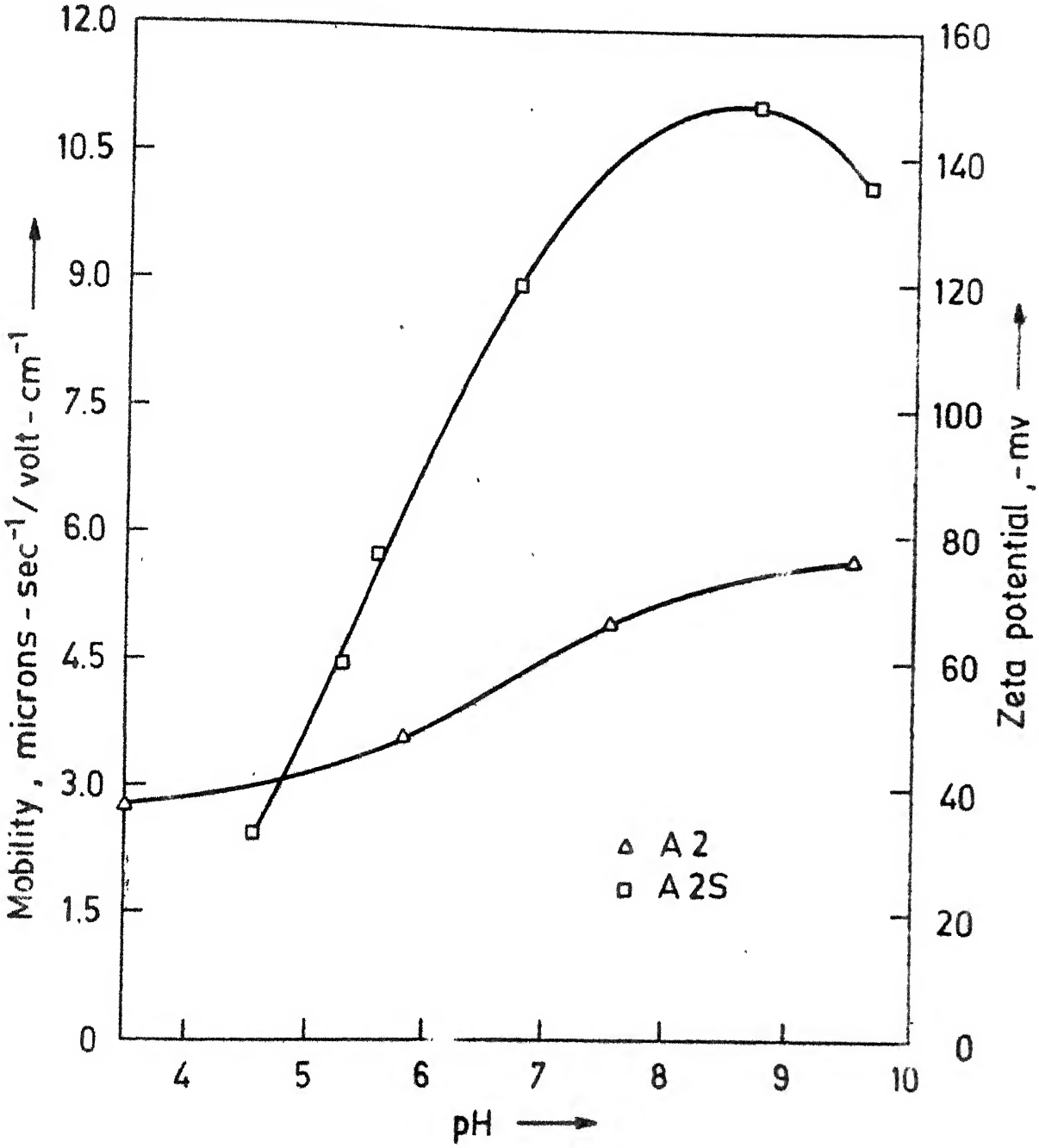

Fig. 4·7 Graph of mobility , zeta potential - pH for Al_2O_3 .

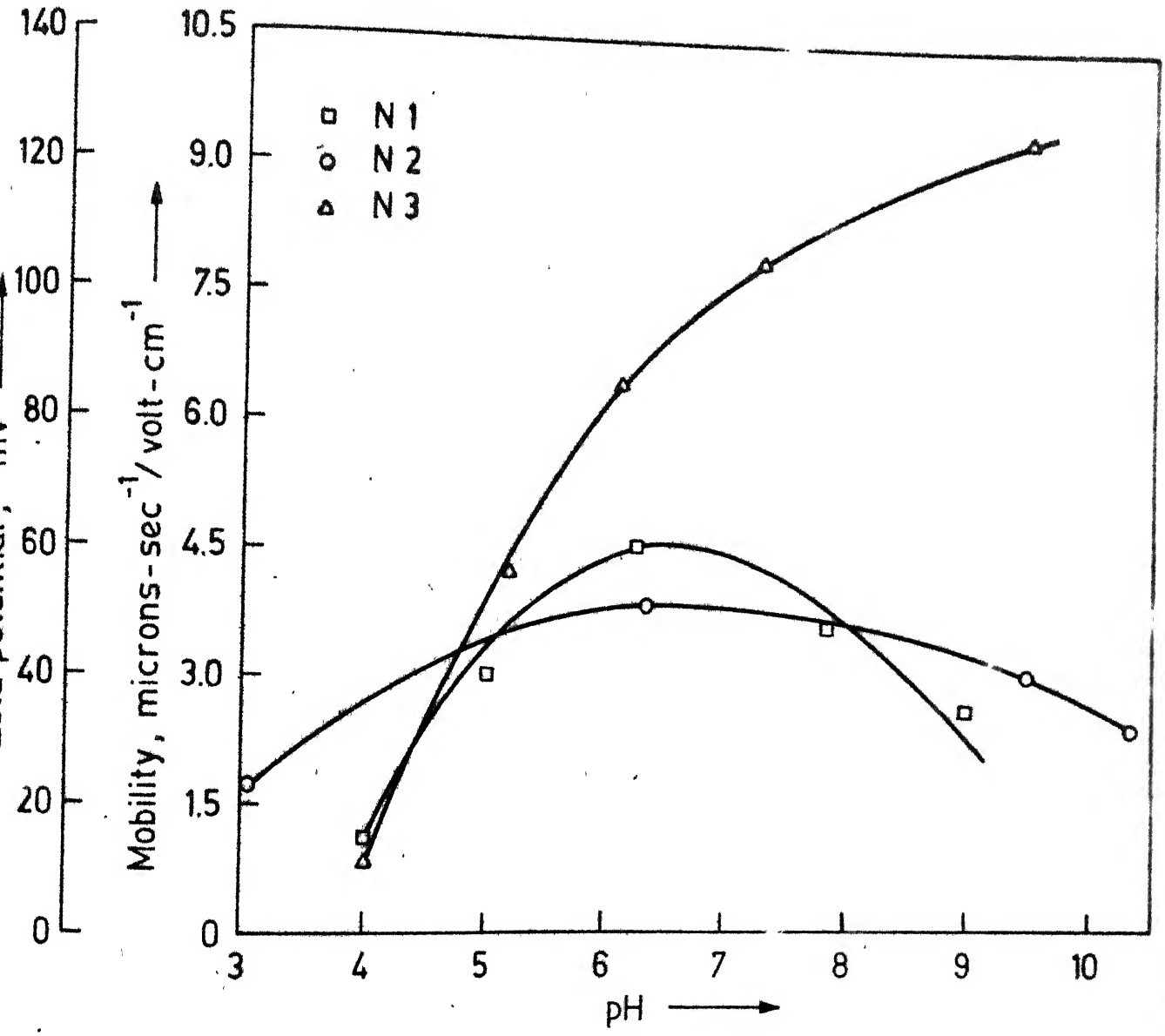

Fig. 4.8 – Graph of mobility and zeta potential vs pH for three different samples of NiO.

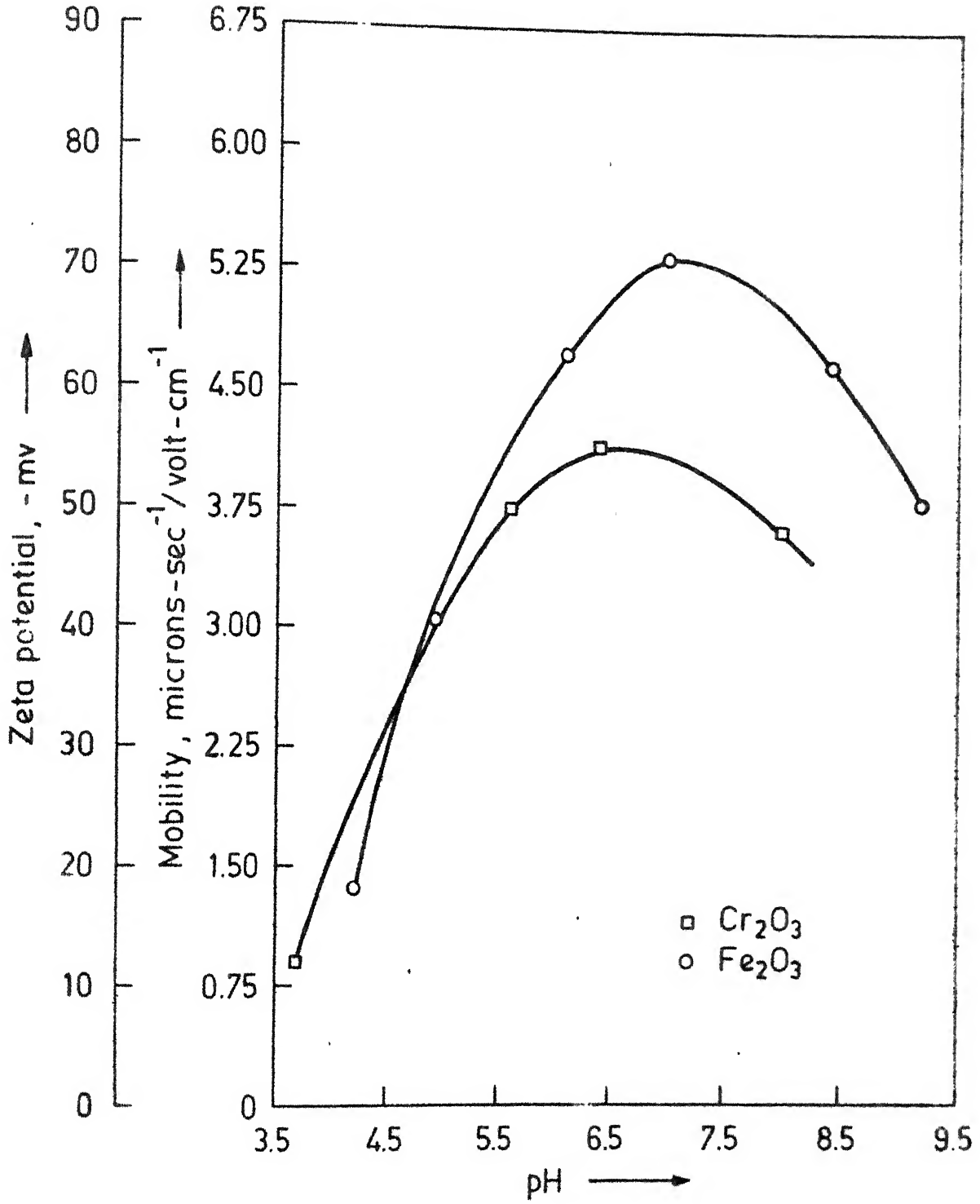

Fig. 4.9 – Graph of mobility and zeta potential vs pH for Cr_2O_3 and Fe_2O_3.

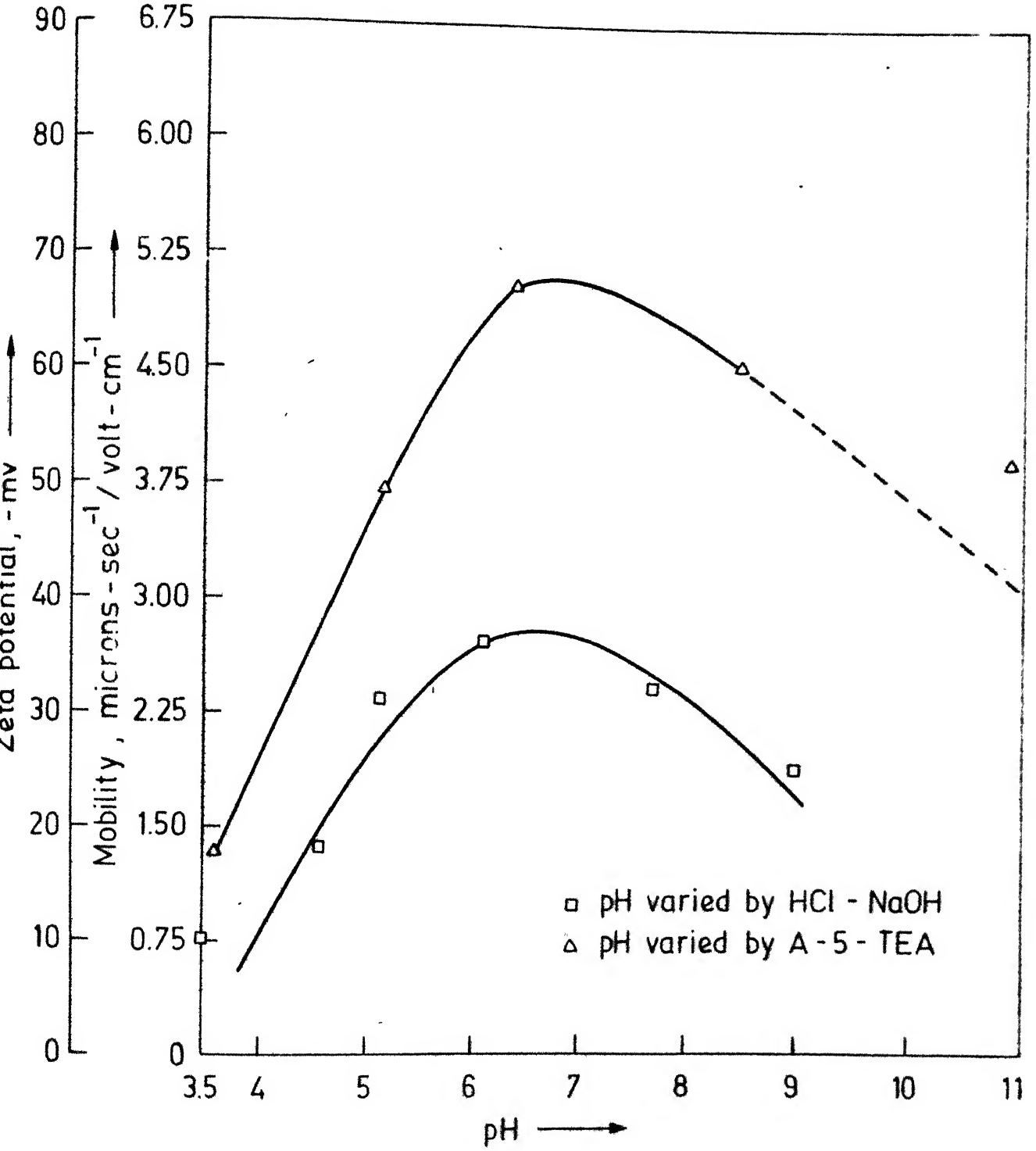

Fig. 4.10- Graph of mobility and zeta potential vs pH profiles for TiO_2.

4(D)

EXPERIMENTAL WORK

Electrode Assembly

The electrode assembly consisted of two rectangular cathodes, made up of mild steel and one anode. The anode was also a rectangular conducting plate on which the coating was desired. In some experiments, 18:8 stainless steel plates were taken as anode while in others, graphite plates were used as anode. The distance between the anode and each cathode was maintained as 3.4 cm approximately. The electrode assembly and the circuit diagram have been shown in Figure 4.11 and 4.12 respectively.

Cathodes and steel anodes were washed in 5% orthophosphoric acid solution for 10 minutes at 70°C, then thoroughly rinsed in distilled water and then in acetone. Graphite anodes were first polished upto 3/0 emery paper and further with linen cloth to give shining and smooth surface. Later on, these plates were boiled in distilled water, dried in an oven at 100°C and then further cleaned with acetone.

Electrophoretic Bath

Like many oxides, the individual alumina particles do not get dispersed in a vehicle. Usually they form suspension of agglomerates [7]. The agglomerate size depends upon the (i) percent powder weight concentration (PWC), (ii) the nature of dispersing medium and dispersing agent, and (iii) pH of the

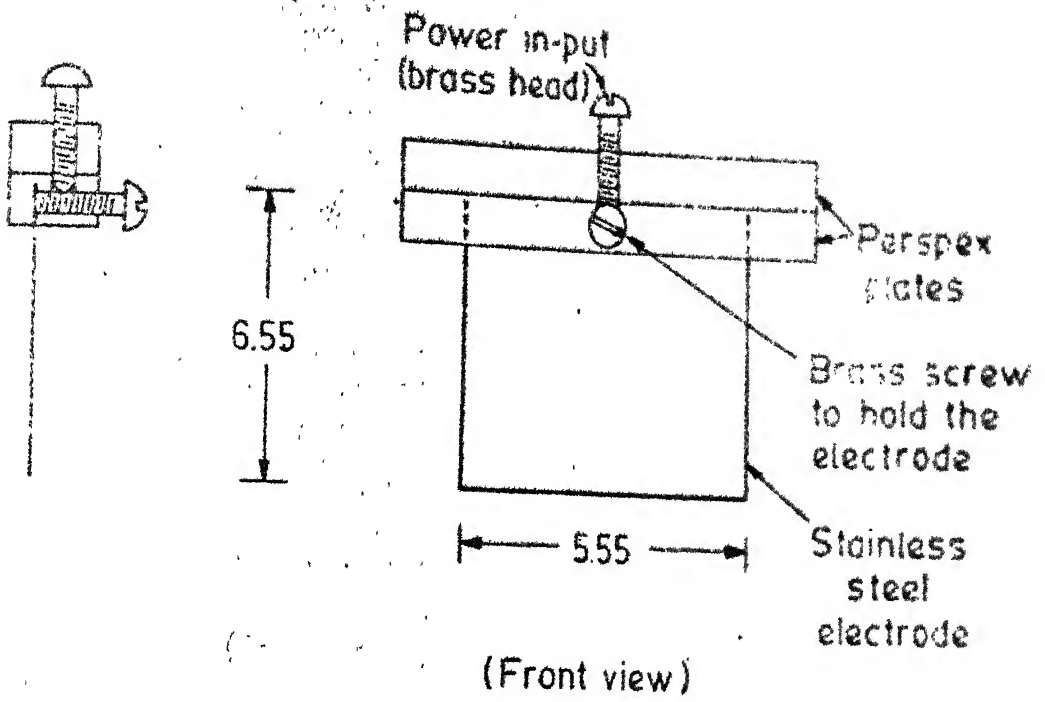

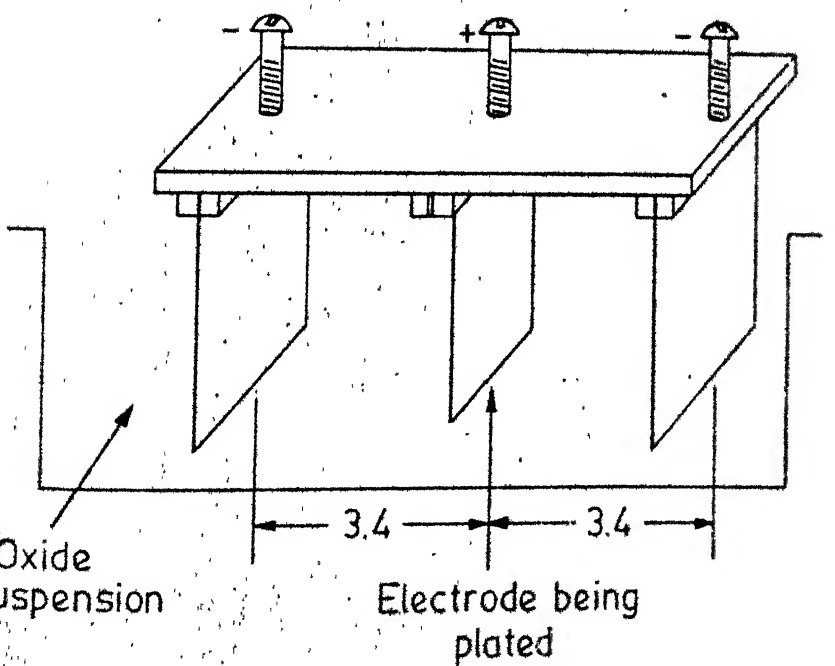

Dimensions in cms.

Fig. 4.11- Electrophoretic cell arrangement for deposition on rectangular electrodes

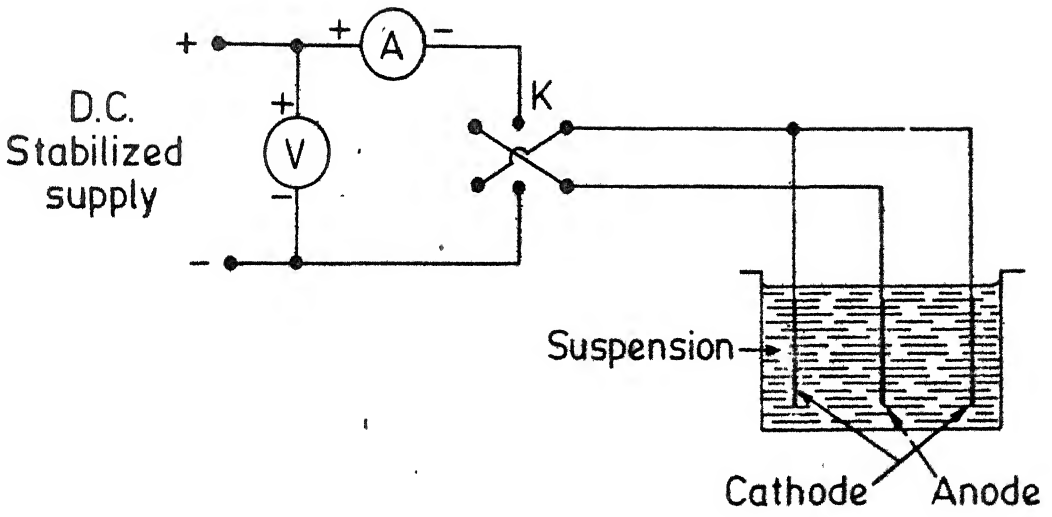

Fig 4·12 - Circuit diagram for electrophoretic deposition.

suspension.

In the present experiments, the bath was prepared in aqueous (deionized water) medium. The aqueous bath is safer in comparison to organic baths as later one pose safty problems inherent in the process.

To obtain stable suspension of alumina powder in water, dispersing agents such as resins, malamines, viscous oils, glues and waxes were available. In the present investigation, the polyacrylic acids from two sources, one synthesized in laboratory and the other imported from Rohm and Haas Company, Philadelphia (USA) were used. The properties of imported polyacrylic acid (Acrysol - 5) are shown in the table 4.1. The properties of synthesized polyacrylic acid have already been discussed in Chapter 3.

The addition of polyacrylic acid to the suspension makes it acidic. Thus, to adjust the required pH in the alkaline region, an organic base, triethylamine $(C_2H_5)_3N$ was added to the suspension.

Deionized water (DI water) was prepared in I.A.C. water plant using mixed bed resin dimineralizer. The specific conductivity of DI water was between 0.5 to 1.0 micro-mhos.

Table 4.1

Polymer concentration	25 percent
pH (5% aqueous solution)	approx. 2
Dissolution with water	Infinite
Molecular weight	Less than 300,000
Brookfield viscosity	
5% concentration	20 cps
25% concentration	18,000 cps

Electrophoretic Deposition

Since electrophoresis is extremely sensitive to the various parameters of electrophoretic bath like pH, conductivity, viscosity, mobility, zeta potential,percent weight concentration of powder, solid : Polyacrylic acid ratio, time of deposition, voltage and current used for deposition, it was necessary to establish the optimum conditions to obtain smooth, uniform and coherent coatings for the present situation.

Experiments were performed in two batches. In first batch, AR grade alumina (supplied by Alcoa Ltd., USA) and Acrysol-5 (Rohm and Haas Company, Philadelphia) were used and alumina coatings were obtained. In second batch of experiments, amorphous alumina and polyacrylic acid (polymer) developed in laboratory [Chapter 2, Chapter 3] were used and coatings of

alumina were obtained. The coatings, obtained from Alcoa-alumina are named as A-type and those obtained from amorphous alumina are called as B-type coatings. The optimum conditions for both these alumina seems to be same and are given below in the Table 4.2.

Table 4.2

Alumina	3.2 percent powder weight concentration
Alumina : Polymer	8 : 1
pH of bath	7.5 - 8.2
Time of deposition	90 seconds
Voltage	30 Volts
Current	40 mA

Deposition of Al_2O_3 - MgO

It has been found that addition of 0.25% MgO to Al_2O_3 improves the sintering properties of alumina coatings and lowers the sintering temperature considerably. It was therefore tried to codeposit Al_2O_3 and MgO in proper proportion electrophoretically. However, the preliminary study on coating behaviour of Al_2O_3 - MgO bath revealed that deposition of thick and uniform coating is almost impossible. The reason being the increase of ionic conductivity of bath by 4 to 5 times due to addition of MgO. This leads to excessive gas evolution and

thereby the detonation of coatings. Figure 4.14 & 4.15 show the increase in specific conductivity of pure deionized water and deionized water containing Al_2O_3 + MgO.

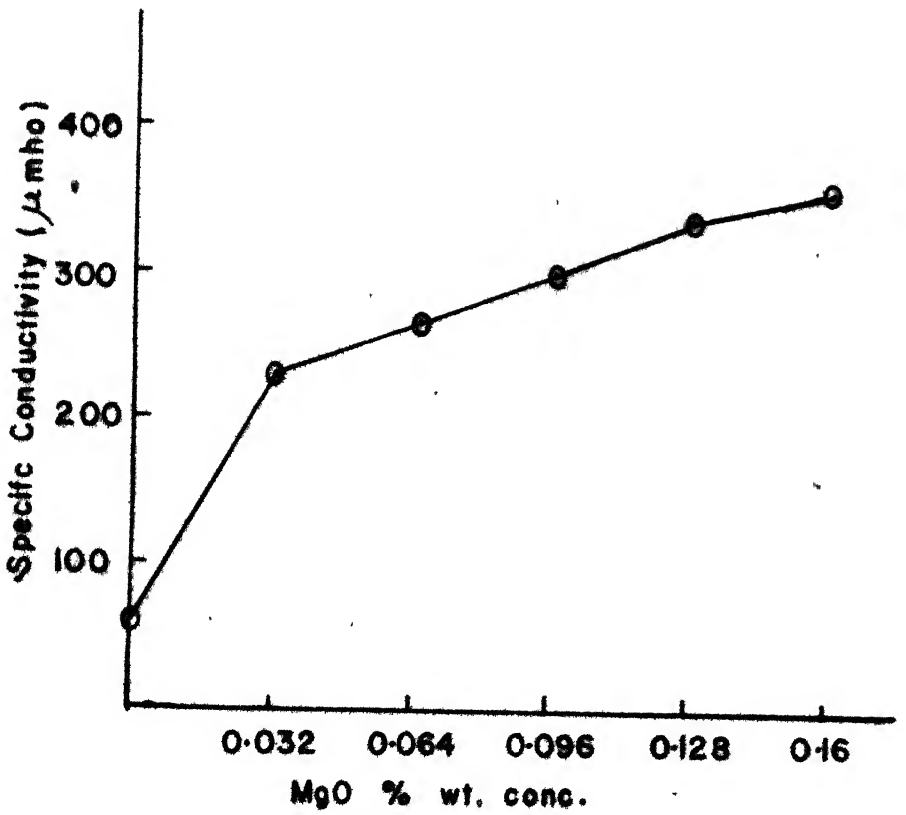

Fig. 4·14 – Effect of addition MgO on sp. conductivity of deionised water.

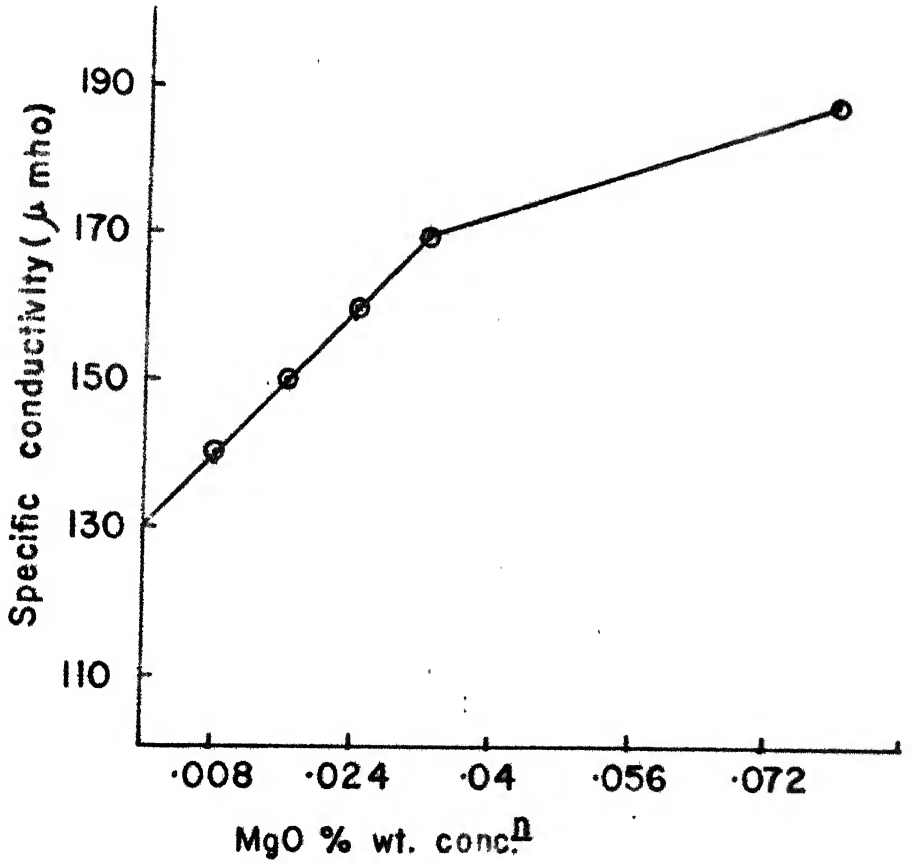

Fig.4·15- Effect of addition of MgO on sp. conductivity Alumina suspension

4(E)

OBSERVATIONS

Alumina coatings of the order of 0.5 mm thickness were obtained on graphite as well as on stainless steel plates. These were quite uniform, smooth and cohrent and white in colour. There were absolutely no cracks and porosity.

Some coatings were tried on heat treated graphite plates (heated to 1500°C in Argon atmosphere) for 30 minutes. The purpose of the heating of plates before deposition was to get rid off the moisture and other gaseous consituents inside the plates.

A dried coating on graphite at a magnification of 100X is shown in Figure 4.17.

Figure 4.18, 4.19 and 4.20 are the magnified views of the coatings, deposited on fired plates of graphite. In third case, coated plate had been dipped in 0.1N $Mg(NO_3)_2$ solution to fill the pores with this solution.

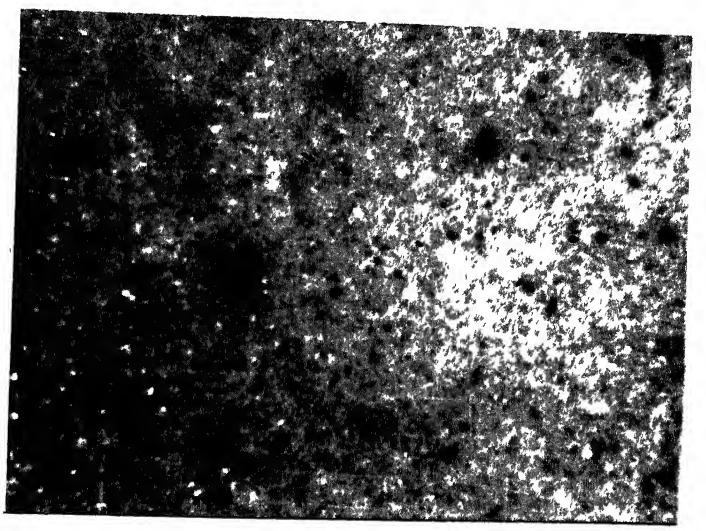

Fig. 4.17 Alumina coated on graphite plate (X 100).

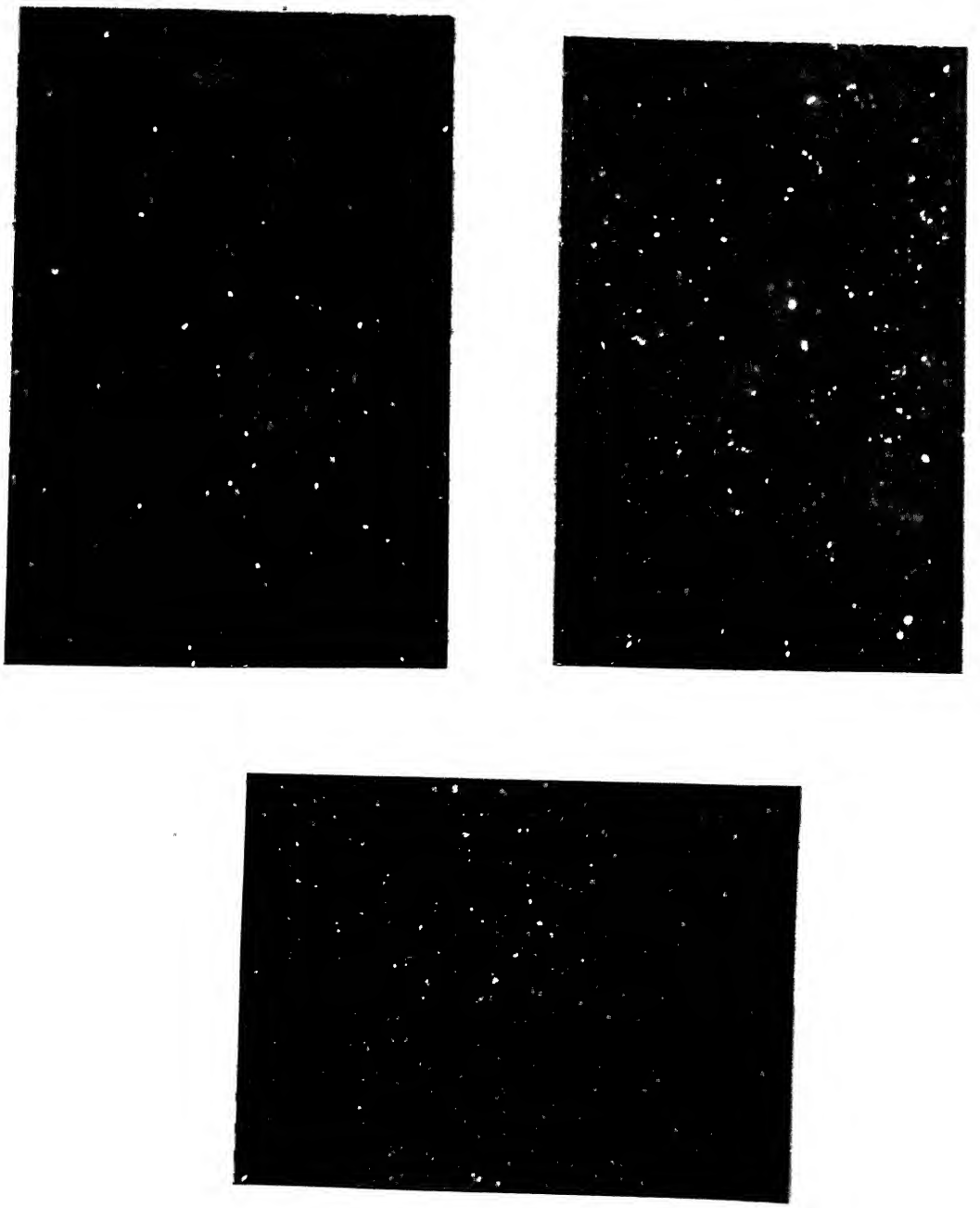

Fig. 4.18-4.20 Alumina coating on fired graphite plates (X 100).

4(F)

POST-TREATMENT OF COATINGS

Coatings (A-type) were dried in air for 24 hrs. and then they were fired on 1600°C for one hour in Induction Melting Unit in Argon atmosphere.

Figure 4.21-4.24 are the magnified views (X 100) of fired coatings. It was found that on this temperature, sintering of alumina did not occur but Adherence of coatings was very good. There appears to be shrinkage in the coatings leading to cracks but in some cases, cracks and fractures are noticed.

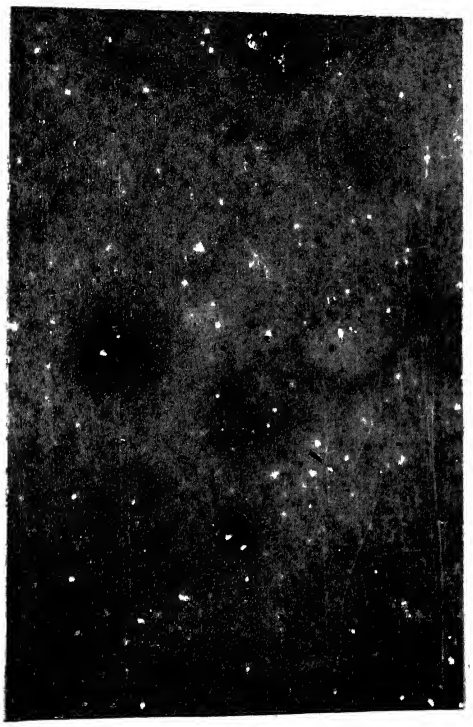

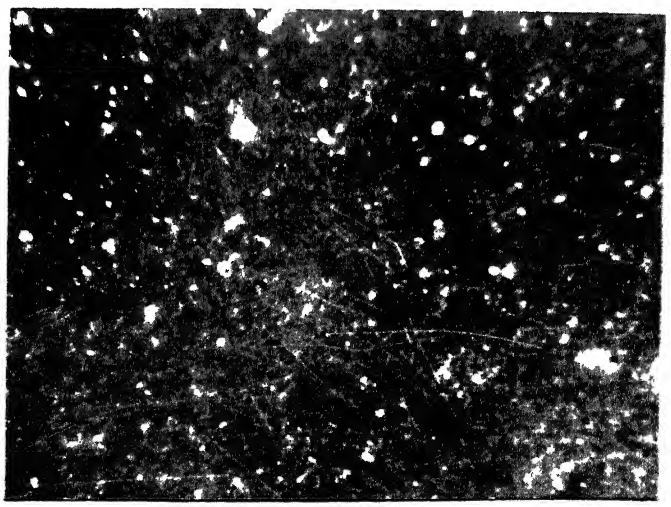

Fig. 4.21-4.23 Fired alumina coating on graphite plates (x 100).

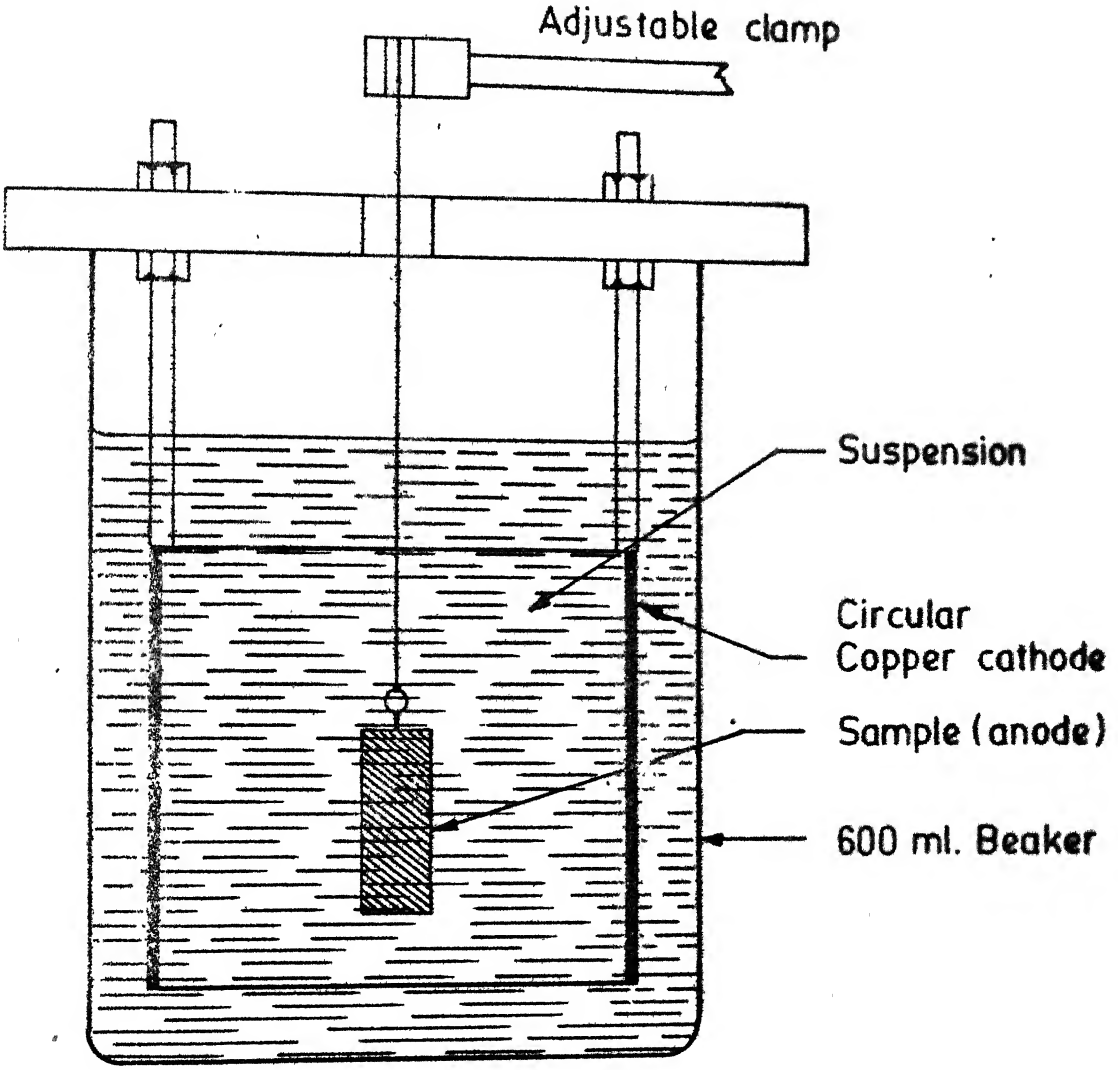

Fig. 4·25 Electrophoretic cell arrangement.

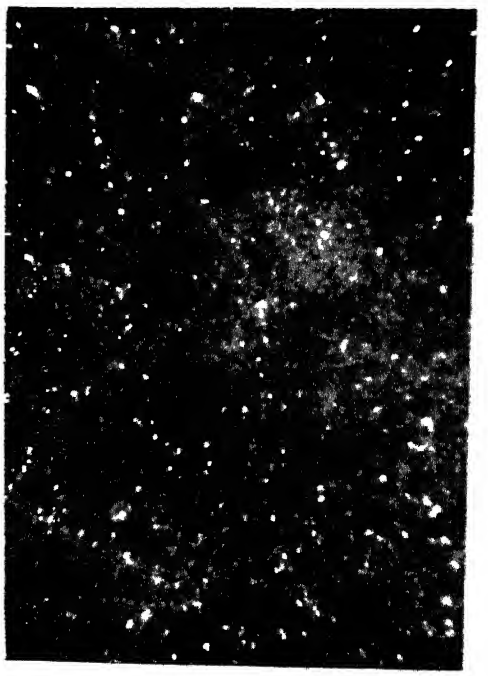

Fig. 4.26-4.28 Fired alumina coating on graphite rods (X 100).

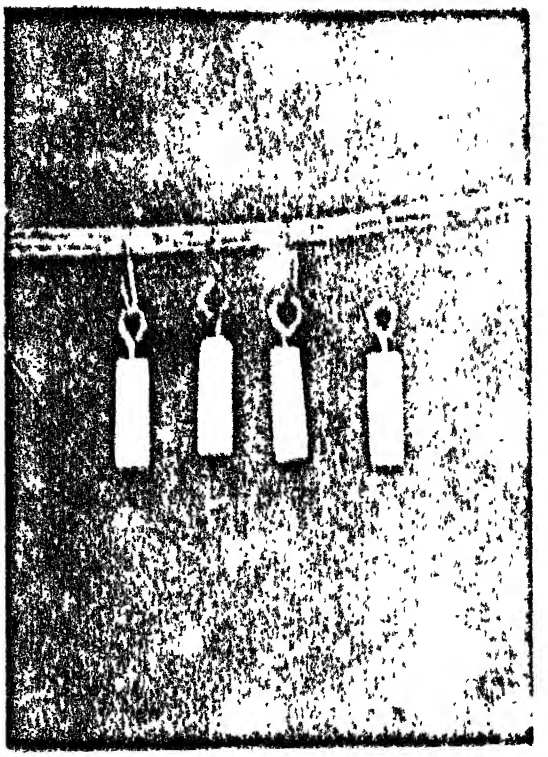

Figure 4.29-Coated graphite rods.

REFERENCES

1. James J. Shyne and G. Howard Scheible, Modern Electroplating, T_s Section.

2. J. Benjamine and A.B. Osborn, Trans. Faraday Soc., No. 36, 287 (1940).

3. S. Senderoff and W.E. Reid, Jr., U.S. Patent 2, 843, 541 (1958).

4. A.C. Werner and R.J. Abbson, Preparation of Protective Coatings by Electrophoretic Methods, WADC Tech. Report 58-11, (Feb. 1958).

5. J.M. Andrews, A.H. Collins, D.C. Cornish and J. Dracass, Proc. Brit. Ceram. Soc., Vol. 12, 211 (1969).

6. R.W. Powers, J. Electrochem. Soc., Vol. 122, No. 4, 490, (1975).

7. W.F. Caley, Electrophoretic Deposition of Metallic Oxides and Production of a Composite Stainless Steel by High Temperature Reduction, Ph.D. Thesis, University of Toronto, (1972).

8. H.S. Fisch, J. Electrochem. Soc., Vol. 119, No. 1, 57, (1972).

9. A.S. Kucharski, Deposition of Tungsten Carbide Surface Coatings, Toronto University (1972).

10. S. Glasstone, An Introduction to Electrochemistry, D. Van Nostrand Company, New York (1975).

11. S. Glasstone and D. Lewis, Elements of Physical Chemistry, D. Van. Nostrand Company Inc., New York.

12. A.K. Biswas, Surface Phenomena in Chemistry and Metallurgy, Deptt. of Met. Engg., I.I.T., Kanpur (1970).

13. D.J. Shaw, Electrophoresis, Academic Press Inc., (1969).

14. N.K. Adam, The Physics and Chemistry of Surfaces, Oxford University Press, (1941).

15. Alexander and Johnson, Colloid Science, Oxford University Press, (1949).

16. J.Y. Choudhary, Electrophoretic Deposition of Metallic Oxides From Aqueous Suspensions, M.Tech. Thesis, Deptt. of Met. Engg., I.I.T., Kanpur, (1978).

CONCLUSIONS

The present work, which consists of synthesis of polyacrylic acid, amorphous alumina and their use in electrophoretic coating on metallic and graphite substrata leads to following conclusions:

1. It is possible to synthesize polymeric acrylic acid using Benzoyl peroxide as catalyst. These polymers with desired molecular weight can be synthesized by changing monomer concentration (acrylic acid) in water and duration of polymerization.
2. Aluminium isopropoxide, similarly, can be synthesized in moderate quantity for production of amorphous alumina in Killogramic quantities easily. During dehydration process, aluminium hydroxides loose water in different steps leading to well defined peaks in DTG and DTA plots and the final product after 500°C is amorphous alumina.
3. The amorphous alumina is fairly stable below 700°C and it needs large activation energy (17 K cal./mole) to crystallize above 700°C.
4. On heating, amorphous alumina transforms to various forms of crystalline alumina. The α-alumina was found to be high temperature phase with chi-, eta- and gamma-forms as intermediate states.
5. The pressed powder in the form of pellets show sintering when heated at or above 1000°C, but it remains incomplete upto 1400°C. The rate of densification can be expressed by Arrhenins equation.

6. The compressive fracture strength of partially sintered pellets were found increasing rapidly with sintering temperature. The maximum strength was found to be 43.28 Kg/mm^2 for pellets sintered at 1400°C.

7. Amorphous alumina powder, when suspended in dilute polyacrylic acid aqueous suspension, get easily deposited electrophoretically on substrata (Anodes).

SUGGESTIONS

1. The polyacrylic acid need addition of suitable inorganic base (e.g. NaOH) for better coating results, as satisfactory coating could not be obtained with pure acrylic acid.

2. Enthalpy and Activation Energy, associated with dehydration peaks, could not be determined. For it, samples with different heating rates should be analyzed thermally.

3. Also, the Kinetics of dehydration could be investigated by electron microscopic studies of hydroxide sample at temperatures corresponding to DTG and DTA peaks.

4. The value of pre exponential factor and that of activation energy for sintering reported in the present work is at higher side because the sintering effect during period when furnace was brought from room temperature to desired temperature has been neglected. Even if this was done these values do not help in understanding the exact process Kinetics because of the complexity of the problem. Thus other independent methods of investigation are required.

Interplanar Spacings and Relative Line Intensities, Filtered CuK Radiation.

Gibb-① site		Bayer-① ite		Nord-② strandite		Boehm-③ ite		Dia-③ spore		Chi④		Gamma④		Eta④		Delta④		Delta④		Theta④		Iota④		Kappa④		Alpha③	
4.82	100	4.72	100	4.790	10	6.11	100	4.71	13							5.02	3	7.97	8	5.2	3	5.45	100	6.2	3	3.479	74
4.34	40	4.36	70	4.373	2	3.164	65	3.99	100					4.6	4	4.55	3	6.58	10	4.5	6	3.47	90	4.5	2	2.552	92
4.30	20	3.19	25	4.310	4	2.346	53	3.214	10							4 07	2	5.07	20	3,53	2	2.92	40	4.2	1	2.379	42
3.35	10	3.08	1	4.205	4	1.980	6	2.558	30					2 8	2	2.87	4	4.05	20	2.85	8	2.72	80	3.04	4	2.165	1
3.31	6	2.69	3	4.153	4	1.860	32	2.434	3			2.7	2			2.73	8	3.56	7	2.72	8	2.59	70	2.79	6	2.085	100
3.17	8	2.45	3	3.880	3	1.850	27	2.386	5							2.58	3	3.40	10	2.56	3	2.46	10	2.70	2	1.740	43
3.08	4	2.34	6	3.600	3	1.770	6	2.356	8	2.40	4	2.41	6	2.40	6	2.43	6	3 28	15	2.43	8	2.34	40	2.57	8	1.601	81
2.44	15	2.28	3	3.462	2	1.662	13	2.317	56	2.27	2	2.28	6	2.27	3	2.28	4	3.21	10	2.31	6	2.24	80	2.41	3	1.546	3
2.42	4	2.21	67	3.022	2	1.527	6	2.131	52			2.18	2					3.03	10	2.24	6	2.15	60	2.32	4	1.510	7
2.37	20	2.14	3	2.815	2	1.453	16	2.077	39	2.11	3	2.09	1					2.783	30	2.11	1	1.99	10	2.26	1	1.404	32
2.28	4	2.06	2	2.706	1	1.434	9	1.901	3	1.98	2	1.98	10	1.97	8	1.99	8	2.737	30	2.01	8	1.94	10	2.16	1	1.374	48
2.23	6	1.97	3	2.490	1	1.412	1	1.815	8			1.95	6			1.95	3	2.593	70	1.91	4	1.88	40	2.11	8	1.276	2
2.15	8	1.91	1	2.478	3	1.396	2	1.733	3							1.91	2	2.457	70	1.80	3	1.73	50	2.06	3	1.289	16
2.03	12	1.83	1	2.451	2	1.383	6	1.712	15							1.80	2	2.311	40	1.73	1	1.61	40	1.99	4	1.190	6
1.98	10	1.76	1	2.390	7	1.369	2	1.678	3	1.53	1	1.54	2			1.54	4	2.277	30	1.61	2	1.55	70	1.95	2	1.160	1
1.95	2	1.71	26	2.261	7	1.312	15	1.633	43					1.52	2	1.51	3	2.156	25	1.54	6	1.492	30	1.87	6	1.147	4
1.90	7	1.68	2	2.217	1	1.303	3	1.608	12							1.49	4	1.989	70	1.49	4	1.461	40	1.82	3	1.138	1
1.79	10	1.64	1	2.029	1	1.224	1	1.570	4							1.45	3	1.950	65	1.45	4	1.435	10	1.74	2	1.125	5
1.74	9	1.59	4	2.013	5	1.209	2	1.522	6					1.40	10	1.40	6	1.793	7	1.43	1	1.410	10	1.64	6	1.099	6
1.67	9	1 56	2	1.898	5	1.178	3	1.480	20	1.39	10	1.39	10			1.39	10	1.791	4	1.40	6	1.370	10	1.54	1	1.083	3
1.65	3	1.55	4	1.777	4	1.171	1	1.431	7							1.29	2	1.[illegible]	10	1.39	10	1.346	40	1.49	3	1.078	7
1.63	1	1.52	1	1.717	1	1.161	3	1.423	12							1.26	1	1.[illegible]	15	1.34	1	1.325	5	1.45	3	1.043	13
1 58	3	1.48	1	1.698	1	1.134	5	1.400	6					1.21	1			1.[illegible]	10	1.29	3	1.288	60	1.43	8	1.018	1
1.57	1	1 47	1	1.680	1	1.092	1	1.376	16			1.14	3	1.14	2	1.14	2	1.[illegible]	20	1.26	2			1.39	10	.998	11
1 55	2	1.45	7	1.667	1	1.046	2	1.340	5			1.04	1	1.03	1			1.[illegible]	8	1.23	2			1.34	3	.982	2
				1.647	2													1.407	60								
				1 591	2													1.392	100								
				1.569	2													1.250	4								
				1,545	2													1.238	9								
				1.510	3													1.180	4								
				1 475	3													1.134	10								
				1 438	6																						
				1.400	2																						

① Typical diffractometer patterns, scanning speed 1 degree per minute (Stumpf, unpublished)
② Papée, Tertian and Biais
③ Swanson and Fuyat, prepared for ASTM X-ray Powder Data File
④ Film patterns, intensities estimated visually (Stumpf)
⑤ Rooksby (1958)
*These pairs of lines occur in positions corresponding with the 400 and 440 lines for the cubic γ-structure.